

Self-Improvement Can Self-Regress: The Rise-and-Collapse Failure Mode of LLM Self-Training

Jianzhe Lin^{1,*}

¹MetaAI

*Work done at Meta

Self-improvement can self-regress. In REINFORCE post-training for code, a model can improve rapidly on the very metric it optimizes and then collapse within the same training campaign. We document this failure mode in a controlled, multi-seed testbed: Qwen-2.5 at 3B and 7B, trained on competitive-programming tasks with binary CodeGrader reward over 10 sequential 20-step campaigns. Across campaigns, pass@1 exhibits a robust *rise-then-collapse*: it climbs to a peak in tens of gradient steps and then falls back, sometimes to near zero. This is not catastrophic forgetting across tasks; it is within-task policy over-optimization on a fixed distribution, and KL- and EWC-style parameter-level constraints do not prevent it.

The operational question is then: *where should the control loop sit?* We compare three intervention levels on the same testbed with bootstrap 95% CIs. **CARE** is a deliberately specified stress test of *between*-campaign memory: a capability posterior, multi-action transfer gate, and regression-aware belief revision. **ES** is a deployed *within*-campaign early-stop rule that rolls forward the peak checkpoint and sets the next campaign’s budget to peak_step+3. **GRPO** changes the underlying RL update rule, using group-relative reward normalization rather than vanilla REINFORCE.

The answer is **regime-dependent**. At **Qwen-2.5-3B**, where naive REINFORCE is fragile, CARE v2 nearly doubles mean end-of-chain pass@1 from 4.9% to **9.5%** (paired bootstrap 95% CI of the per-seed difference [+0.4, +8.9], excludes zero, $n=5$, positive in 4/5 seeds); it also beats ES (8.2%, $n=5$). At **Qwen-2.5-7B**, CARE reaches parity with naive REINFORCE (13.8% vs 11.8%), while ES reaches **22.2%** [14.1, 28.0] ($n=3$). However, out-of-the-box **GRPO** reaches **20.7%** [15.7, 25.1] ($n=5$) without any campaign-level orchestration, nearly matching orchestrated REINFORCE+ES; adding CARE on top of GRPO remains at parity (20.4% [10.9, 28.6], $n=5$).

GRPO raises the floor, but does not remove the cliff. Per-step trajectory diagnostics show that GRPO’s 7B gain comes from improved *between-campaign* carryover, not from within-campaign stabilisation: the per-campaign peak-to-end gap is ≈ 17 pt under both REINFORCE and GRPO. A deployed GRPO+ES run gives mixed evidence: 2/3 seeds improve over naive GRPO, but one final-campaign cliff drives the 3-seed mean to 17.0% [0.0, 28.1], showing that even algorithm-level and within-campaign control together do not eliminate single-campaign collapse. A single-seed Gemma-3-4B pilot shows the same qualitative rise-then-collapse signature on the identical CodeGrader testbed (peak 32.8%, end 0%); we report this as a pilot data point, not a multi-seed replication, but it suggests the phenomenon is not confined to the Qwen family.

Date: June 23, 2026

Correspondence: Jianzhe Lin at jianzhelin@meta.com



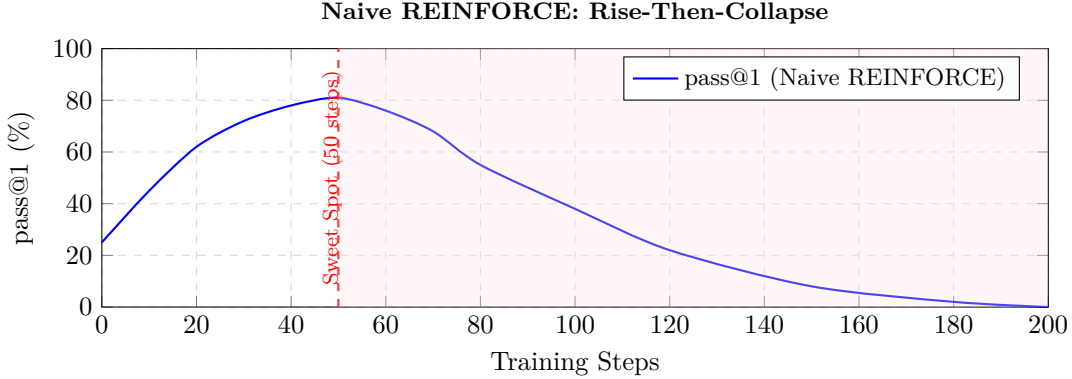


Figure 1 Rise-then-collapse in naive REINFORCE training (Qwen-2.5-7B on competitive programming): pass@1 rises from 25% to 81% in the first 50 steps, then degrades to near-zero by step 200. Self-improvement is also, on its own target metric, self-regression. *This is a diagnostic single 200-step run from one seed used to characterise the shape of the trajectory; the same rise-then-collapse pattern is shown across multiple seeds and both 3B and 7B scales in Figure 3 (chained 20-step campaigns) and quantified in Section 6 (phase-transition score, onset step, post-onset latency).* The remainder of the paper compares interventions *between* campaigns (CARE), *within* a campaign (deployed early-stop, ES), and at the *algorithm level* (GRPO; Section 5.9) for keeping end-of-chain pass@1 above this collapse.

1 Introduction

Self-improving AI systems are proliferating: iterative DPO (Xu et al., 2024; Pang et al., 2024), self-play (Singh et al., 2024; Chen et al., 2024), self-reward training (Yuan et al., 2024), STaR (Zelikman et al., 2022), and autonomous research agents (Lu et al., 2024) all aim to make models better by learning from their own outputs. The promise is a virtuous cycle: the model improves, generates better data, and improves further.

But self-improvement is not a free lunch. Concurrent work on RLVR (reinforcement learning with verifiable rewards) has begun to surface a closely related failure mode: policy entropy collapses, exploration shrinks, and the same RL update that initially improved the model later destroys it (Anonymous, 2026b; Authors-TBD-from-arXiv-2602.09782, 2026; Anonymous, 2026a). We document the same effect from a different angle — a within-campaign *rise-then-collapse* on a binary CodeGrader reward — and ask which level of intervention actually moves end-of-chain pass@1 once it appears.

Consider a concrete failure mode. An autonomous research agent discovers that increasing the rejection sampling ratio from $4\times$ to $16\times$ improves pass@1 on code generation by 6%. Encouraged, it applies the same strategy to the next campaign. But this time, the strategy *also* reduces solution diversity by 4% and degrades hard-case accuracy by 1%—regressions invisible to the agent because it only tracked the target metric. Over repeated campaigns, the model becomes narrowly optimized: high on its target metric but brittle, homogeneous, and fragile on distribution shifts.

This is not a hypothetical. We observe it directly in our REINFORCE training experiments (Figure 1): when training Qwen-2.5-7B on competitive programming tasks, pass@1 rises from 25% to 81% within the first 50 gradient steps—then *collapses to near-zero by step 200*. The model improves rapidly, then catastrophically forgets how to generate correct code. This “rise-then-collapse” pattern is the within-campaign manifestation of the same phenomenon: naive optimization without memory or constraint accumulates hidden damage that eventually overwhelms the gains.

What the collapse is, and is not. The collapse is *not* primarily caused by task switching. It occurs within a nominally fixed competitive-programming training distribution, with no change of dataset or objective. We interpret it as *within-task policy over-optimization*: early REINFORCE sharpens useful behaviours already present in the pretrained model, but continued optimization narrows the policy around brittle reward-correlated patterns, reducing solution diversity and overwriting broad code-generation priors. The model can self-regress without any task change. This distinguishes our setting from the catastrophic-forgetting literature (where forgetting is induced by switching tasks), and the magnitude of each campaign’s collapse—together with how

much of the within-campaign peak the chain retains—turns out to be scale-dependent. Sections 5–6 measure that scale dependence and trace it to three structural properties of the per-step trajectory.

More broadly, we show empirically (Section 5.12) that naive self-improvement pipelines consistently improve their target metric while causing hidden regressions on secondary capabilities—a phenomenon we call **capability regression through scalar optimization**.

The Core Insight. We observe that improvement strategies are not scalar operators (“+0.06 on pass@1”) but *capability tradeoff operators*—they shift an entire vector of capabilities:

$$s : \mathbf{c} \mapsto \mathbf{c} + \delta_s(\mathbf{c}, \text{ctx}) \quad (1)$$

where \mathbf{c} is a K -dimensional capability vector and δ_s is the strategy’s *capability effect*, which depends on the current capability state and context. A self-improving system that remembers only “this strategy improved the score” is discarding most of the information it needs to improve safely and cumulatively.

Our Approach: CARE. We introduce **Capability-Aware Research Experience (CARE)**, a meta-scientific memory system with three modules:

1. **Capability-Effect Memory** records each strategy’s full capability delta, boundary conditions, and confidence.
2. **Self-Improvement Transfer Gate** decides whether to reuse, adapt, pilot, or reject a past strategy—maximizing target improvement subject to no hidden regression on protected capabilities.
3. **Regression-Aware Belief Revision** updates memory when a strategy’s observed effects violate predictions, enabling the system’s self-improvement policy to itself improve over time.

The paper’s central question is operational: **where should the control loop sit** when a self-improving REINFORCE run keeps collapsing? We study three levels of intervention at three different timescales. **Between-campaign** control (CARE): after each campaign, decide what to keep and what to roll back via a capability-aware memory and gate. **Within-campaign** control (ES): during each campaign, watch the per-step trajectory and stop in time. **Algorithm-level** control (GRPO (Shao et al., 2024; Guo et al., 2025)): change the RL update itself, so the underlying loss is less prone to collapse in the first place. These act at different timescales (after a campaign, during a campaign, and inside each gradient step) and exploit different signals; we ask which one actually moves end-of-chain pass@1 in our testbed.

Contributions.

1. **Rise-then-collapse under verifiable-reward REINFORCE.** On Qwen-2.5 3B and 7B trained with REINFORCE and binary CodeGrader reward, pass@1 rises to a peak in tens of gradient steps and then collapses within the same campaign (Figure 1); chained over 10 campaigns the pattern repeats across multiple seeds and both scales (Figure 3). Parameter-level regularization (EWC-style KL constraints) does not prevent it (Table 1).
2. **Between-campaign memory has a fragile-regime niche.** At Qwen-2.5-3B, CARE v2 nearly doubles mean end-of-chain pass@1 (9.5% vs 4.9%; paired bootstrap 95% CI of per-seed difference [+0.4, +8.9], excludes zero, $n=5$; Table 6) and beats a deployed within-campaign early-stop rule (ES, 8.2%, $n=5$). At Qwen-2.5-7B CARE reaches parity with naive (13.8% vs 11.8%, overlapping CIs and paired CI includes zero); the value of between-campaign memory is bounded to the small-model fragile-signal regime.
3. **Within-campaign stopping sets a higher 7B ceiling under REINFORCE.** The ES condition ($\text{max_steps}(c+1) = \text{peak_step}(c) + 3$, base hyperparameters preserved, peak checkpoint rolled forward) reaches **22.2%** [14.1, 28.0] end pass@1 on Qwen-2.5-7B 10-campaign REINFORCE chains ($n=3$, Table 9), the highest end-of-chain pass@1 of any orchestrated REINFORCE configuration we tested at this scale.
4. **GRPO raises the end-of-chain floor without removing the within-campaign cliff.** Replacing REINFORCE with GRPO (group-relative reward normalization, no algorithmic change to the orchestrator) under *the same* 10-campaign 20-step chain protocol yields **20.7%** [15.7, 25.1] ($n=5$) at 7B from naive

GRPO alone, nearly matching REINFORCE+ES (Table 10). However, per-step trajectory diagnostics on the W4 vs W17 7B A0 chains (Table 11) show that GRPO does *not* close the within-campaign peak-to-end gap: both update rules leave ≈ 17 pt of peak-end gap per campaign. GRPO’s gain instead comes from better *between-campaign* carryover (mean end pass@1 stays at the 20% level across the chain, while REINFORCE’s drifts down). CARE on top of GRPO gives no measurable improvement at $n=5$. This suggests a natural complementarity hypothesis between GRPO and ES (ES still has the within-campaign peak left to recover under GRPO), which W18 (GRPO+ES, $n=3$) only partially supports: 2/3 seeds improve over naive GRPO, but a single final-campaign cliff prevents a statistically separated mean gain.

5. **A two-timescale account of where each level helps.** Self-improving RL on this testbed fails at two distinct timescales — *within* a campaign (cliff-like rise-then-collapse: phase-transition score ≈ 0.78 , onset near step $\approx 17/20$, zero usable post-onset latency for an end-of-campaign gate; Section 6) and *between* campaigns (each campaign’s end checkpoint either carries forward gain or drifts down). The three intervention levels target different cells of this (*within, between*) decomposition: CARE helps fragile carryover at 3B; ES recovers within-campaign peaks under REINFORCE; GRPO improves carryover at 7B but leaves the within-campaign cliff approximately intact.

Positioning relative to prior work. Prior work identifies *what* self-improvement degrades — diversity, OOD generalization, prompt-following, and exploration (Wu et al., 2024; Kumar et al., 2025; Chen et al., 2025; Kumar et al., 2024; Singhal et al., 2025). We instead study *when* degradation becomes actionable inside a chained RL training loop. This temporal structure determines the correct control level: between-campaign memory when the per-step signal is weak, and within-campaign stopping when it is rich. We are explicitly *not* claiming to be the first to observe collapse or self-regression in self-improving LLM training.

2 Related Work

Self-Improving Language Models. Self-play (Singh et al., 2024; Chen et al., 2024), self-reward (Yuan et al., 2024), iterative DPO (Xu et al., 2024; Pang et al., 2024), STaR (Zelikman et al., 2022), and ReST (Gulcehre et al., 2023) optimize a single target metric without tracking capability tradeoffs. SPIN (Chen et al., 2024) frames self-improvement as a game but still uses scalar reward. These methods aim to make self-improvement compound; the question we take up is when and where this compounding fails inside a chained RL training loop, and which intervention level can stop the failure (Section 5).

Self-Improvement Reversal, Reward Over-Optimization, and Exploration Collapse. A growing line of work documents that self-improvement under scalar or self-generated feedback degrades non-target capabilities even when the target metric continues to rise. Wu et al. (2024) call this *self-improvement reversal*: iterative post-training (SFT, DPO, SFT→DPO) raises pass@1 while reducing output diversity and out-of-distribution generalization, and biases the model toward easier problems rather than genuinely harder ones. Kumar et al. (2025) report *template collapse* under prolonged self-consistency-based self-training: large reasoning models learn to ignore the prompt and emit a fixed template answer, which they attribute to the self-reinforcing nature of imperfect feedback. Chen et al. (2025) observe that Pass@1 reward in RLVR pushes the policy toward conservative, similar actions and suppresses exploration, motivating Pass@ k -style reward redesigns that explicitly balance exploration vs. exploitation. Kumar et al. (2024) report behaviour collapse during self-correction RL and prescribe a regularised two-stage training procedure (separating the initialisation that learns a correction strategy from the high-reward fitting that would otherwise overwrite it). Singhal et al. (2025) study binary vs. pass-rate reward design for code-generation RL and find that pass-rate’s early advantage typically disappears with continued training, suggesting that the failure mode is at the level of gradient *direction* rather than reward *density*. Concurrent 2026 work on RLVR makes the same diagnosis at the algorithm level: Anonymous (2026b) characterise “prosperity-before-collapse” under off-policy RLVR with stale data and trace it to entropy collapse; Authors-TBD-from-arXiv-2602.09782 (2026) propose a gradient-preserving entropy controller that targets the same collapse phenomenon; and Anonymous (2026a) reframe RLVR’s clipping schedule as an exploration–exploitation knob. These works treat the cliff as an algorithm-level pathology to be fixed by changing the update rule. We complement that line by treating

the cliff as a fixed empirical phenomenon and asking which level of *control* around the rule actually recovers end-of-chain pass@1. [Authors-TBD-from-arXiv-2603.08660 \(2026\)](#) push RLVR scaling without external labels; whether the rise-then-collapse signature we observe also appears in their unsupervised regime is a natural follow-up. Prior work identifies *what* self-improvement degrades: diversity, OOD generalization, prompt-following, and exploration. We instead study *when* the degradation becomes actionable inside a chained RL training loop, and show that this temporal structure determines the correct control level — between-campaign memory when the per-step signal is weak, within-campaign stopping when it is rich (Sections 5–6).

Autonomous Research Agents. The AI Scientist ([Lu et al., 2024](#)) and FunSearch ([Romera-Paredes et al., 2024](#)) automate experimentation, but treat each experiment independently. They rediscover which strategies work without building persistent memory of *how strategies trade off capabilities*. CARE tests whether the meta-scientific memory absent in these agents would help; our results show this memory is genuinely useful in the small-model regime (Qwen-2.5-3B) but redundant once the per-campaign signal is strong (Qwen-2.5-7B), and an online within-campaign rule dominates at both scales.

Hyperparameter and Strategy Optimization. Bayesian optimization ([Snoek et al., 2012](#); [Balandat et al., 2020](#)) and population-based training ([Jaderberg et al., 2017](#)) search for good configurations but optimize a scalar objective. AgentHPO ([Liu et al., 2024](#)) uses LLMs to reason about hyperparameters but lacks structured memory of capability effects. Multi-objective HPO ([Daulton et al., 2020](#); [Karl et al., 2022](#)) considers multiple objectives simultaneously but does not learn transferable tradeoff knowledge.

Continual Learning and Catastrophic Forgetting. EWC ([Kirkpatrick et al., 2017](#)), SI ([Zenke et al., 2017](#)), and GEM ([Lopez-Paz and Ranzato, 2017](#)) address forgetting of *task knowledge*—the model forgets how to do task A after learning task B. Our setting is distinct: we observe within-task self-regression under continued REINFORCE on a fixed distribution (Section 1, “What the collapse is”), and we test whether a meta-level memory of safe-vs-unsafe improvement strategies can prevent it. Our scale-dependent result (Sections 5–6) is consistent with online within-campaign prediction being the more general ingredient, with campaign-level memory acting as a useful but scale-bounded complement.

Meta-Learning. MAML ([Finn et al., 2017](#)) learns initializations for fast adaptation; Meta-SGD ([Li et al., 2017](#)) learns per-parameter rates. These meta-learn over model parameters. CARE is positioned as meta-learning over the *self-improvement process*—which interventions improve which capabilities and which they regress; whether this is the right level of abstraction is the question we test empirically.

Curriculum Learning and Data Selection. Curriculum learning ([Bengio et al., 2009](#)), self-paced learning ([Kumar et al., 2010](#)), and data mixing ([Xie et al., 2024](#)) select what to train on but treat curriculum effects as scalar improvements. CARE models curriculum strategies as capability tradeoff operators that may help some capabilities while hurting others.

3 Problem: Self-Improvement is Not a Free Lunch

A model’s *capability state* is a vector $\mathbf{c} = (c_1, \dots, c_K) \in [0, 1]^K$ measuring performance on K held-out evaluation axes (e.g., matched-difficulty pass@1, held-out hard pass@1, OOD pass@1). A training strategy s acts as a capability operator: applying s in context $x \in \mathcal{X}$ yields a capability delta $\delta_s(x) \in \mathbb{R}^K$ so that $\mathbf{c}' = \mathbf{c} + \delta_s(x)$. We say s causes *hidden regression* on a protected capability $j \in \mathcal{P} \subseteq [K]$ if $\delta_s^{k^*} > 0$ but $\delta_s^j < -\epsilon$ for the target capability k^* and a threshold ϵ ; that is, the strategy improves the target while silently degrading a protected dimension. Scalar-objective self-improvement accepts any s with $\delta_s^{k^*} > 0$ regardless of δ_s on protected axes, so under any distribution of strategies for which $E[\delta_s^j \mid \delta_s^{k^*} > 0] < 0$ on protected j , the expected protected-capability drift after T campaigns is $-\mu_j T$. We confirm this pattern empirically in Section 5.12: scalar pass@1 improvements on the training distribution do not transfer to held-out hard or non-English splits regardless of training method. *Negative transfer* is the additional risk that a strategy beneficial in one context x_1 becomes harmful in another x_2 , which a memory-free chain cannot detect. Formal

<p>Module 1: Capability-Effect Memory \mathcal{M} Records structured entries: $\{s, \text{ctx}, \delta_s, \text{boundary}, \text{confidence}\}$</p> <p>Module 2: Self-Improvement Transfer Gate \mathcal{G} Input: candidate strategy s, current context x, protected caps \mathcal{P} Output: <code>reuse</code> <code>adapt</code> <code>pilot</code> <code>reject</code> Objective: $\max \mathbb{E}[\delta_s^{k^*}]$ s.t. $\Pr[\delta_s^j < -\epsilon] \leq \alpha, \forall j \in \mathcal{P}$</p> <p>Module 3: Regression-Aware Belief Revision \mathcal{R} Trigger: observed δ_s^{obs} deviates from predicted $\hat{\delta}_s$ Action: update boundary conditions, confidence, and transfer policy</p>
--

Figure 2 CARE architecture. Module 1 stores capability-level effects. Module 2 gates strategy transfer. Module 3 revises beliefs when predictions fail. Together they make self-improvement cumulative and regression-aware.

definitions (Capability Vector, Training Strategy as Capability Operator, Hidden Regression, Regression Accumulation, Negative Transfer) are in Appendix C.

4 CARE as a Diagnostic Foil for Campaign-Level Control

What CARE is, and is not, in this paper. CARE is *not* claimed here as a complete K -dimensional deployed controller for self-improving LLM training. It is a deliberately specified *stress test of the campaign-level intervention class*: the K -dimensional capability vector, Gaussian posterior, and gate routing are written down in full so that “campaign-level memory + gate + belief revision” is a concrete, falsifiable object that subsequent empirical sections can interrogate. The deployed gate in our headline experiments uses only the scalar end/peak pass@1 ratio (i.e. $K=1$; see Section 5.12); the multi-capability formalism below motivates the broader design space and is audited post-hoc, not asserted as a fielded result. Readers who prefer to skip the mathematical specification can read Modules 1–3 below at the level of the architecture box (Figure 2) and then proceed directly to the experimental sections.

CARE consists of three tightly coupled modules that together enable safe, cumulative self-improvement (Figure 2).

4.1 Design Sketch

CARE is the natural memory-and-gating candidate for campaign-level intervention against self-regression. Below we sketch the three modules at the level of detail needed to interpret the experiments; the full mathematical specification (entry tuple, posterior update, gate routing logic, belief-revision Bayesian update, and Algorithm 1 pseudocode) is in Appendix D.

Module 1: Capability-Effect Memory \mathcal{M} . Stores one entry per (strategy, context) pair containing the observed capability delta $\delta_s^{\text{obs}} \in R^K$, a boundary predicate over contexts where the strategy is judged safe, and a confidence score. Multiple observations of the same strategy are aggregated as a linear Gaussian posterior over $\delta_s(x)$ conditioned on context features $\phi(x)$. The intent is a transferable record of *when* a strategy helps or hurts, not just *whether* it improved a scalar metric.

Module 2: Self-Improvement Transfer Gate \mathcal{G} . Given a candidate strategy s and current context x , the gate selects one of four actions $\{\text{reuse}, \text{adapt}, \text{pilot}, \text{reject}\}$ to maximise expected target improvement subject to a per-protected-capability regression-probability constraint. Concretely, we evaluate $\Pr[\delta_s^j < -\epsilon \mid x]$ via the posterior CDF for each protected j and reject any strategy whose worst-case regression probability exceeds a threshold α . In the experiments we implement a simplified hard-rule version (deterministic ratio test on observed end/peak pass-rate). Critically for our negative result: this signal is only computable *at end of campaign*, not during it.

Module 3: Regression-Aware Belief Revision \mathcal{R} . When the observed capability delta deviates from the posterior prediction by more than a Mahalanobis-distance threshold, the system simultaneously refines the strategy’s boundary predicate, updates the Gaussian posterior with inflated noise, and tightens the gate’s regression-probability threshold α . The intent is that the orchestrator’s transfer policy *itself* improves over time as it accumulates surprise events.

Conceptual analysis as a diagnostic foil, not a guarantee (full version in Appendix D). Under idealising assumptions (Lipschitz capability effects, σ_0/\sqrt{m} posterior coverage) the long-run hidden regression rate under CARE would be $\alpha + O(K/\sqrt{T})$ across T campaigns vs. $\Theta(1)$ for a scalar chain, and belief-revision accuracy would grow monotonically with the number of memory entries. We include the analysis not as a deployment guarantee but as a *foil*: it formalises the smooth regime in which campaign-level memory would be expected to help, and the experiments in Section 6 show exactly why REINFORCE LLM training violates that regime (phase-transition score ≈ 0.78 , zero usable post-onset latency). Whether the abstraction holds is itself part of the empirical contribution.

Design intent vs. empirical outcome. CARE is not proposed here as a universally best intervention. It is a deliberately plausible campaign-level candidate used to test whether memory and gating are the right level of control for self-improvement collapse. Section 5 reports a scale-dependent answer: CARE *significantly outperforms naive in the Qwen-2.5-3B fragile regime* (9.5% vs 4.9%; paired bootstrap 95% CI of per-seed difference [+0.4, +8.9] excludes zero, $n=5$) but *does not significantly outperform naive at Qwen-2.5-7B* (13.8% vs 11.8%, overlapping CIs); at both scales the deployed within-campaign ES rule (Section 5.8) reaches a higher ceiling. Section 6 diagnoses why.

Scope of the gate’s signal in this paper. Our deployed CARE implementation uses a *scalar* gate over the end/peak pass@1 ratio (i.e. $K=1$ at training time); the multi-capability vector formalism above motivates the broader class but the cross-language (cpp_acc) and OOD (ood_acc) measurements in Section 5.12 enter only as post-hoc diagnostic evaluations, not as control signals. A post-hoc K-dim audit (Table 15) shows the multi-capability information is non-trivial; extending the deployed gate to a true K-dim posterior is left as future work.

Honest framing of “capability-aware”. The word *capability-aware* in CARE’s name and Section 1 contribution list refers to the framework’s *design space* — the K-dimensional capability operator, the protected-set objective, the Gaussian posterior in Appendix D — not to the deployed gate used in this paper’s headline experiments. What is deployed is the scalar reduction $K=1$ on pass@1, plus the multi-action transfer gate (`reuse/adapt/pilot/reject`) and the regression-aware belief revision, both of which act on that scalar signal. Readers should therefore interpret our 3B positive trend (Section 5.6) as evidence that a *scalar-gated* version of CARE, not a fully K-dimensional one, provides the small-model benefit. Whether activating the K-dim posterior would tighten the 3B effect or extend it to 7B is the single most informative follow-up experiment to the present paper, and we discuss it in the exploratory K-dim audit (Appendix I) rather than over-claim it in the main results.

5 Experiments

5.1 Setup

Testbed. Code generation self-improvement across 5 sequential campaigns: (C1) String Manipulation, (C2) Basic Data Structures, (C3) Advanced Data Structures, (C4) Algorithm Design, (C5) Systems-Level. Problems drawn from HumanEval (Chen et al., 2021), MBPP (Austin et al., 2021), and APPS (Hendrycks et al., 2021). Each campaign: 50 training problems, 30 held-out evaluation problems.

Campaign Length: three distinct settings. The paper uses three deliberately-chosen campaign-length protocols. **(1) Diagnostic 200-step run** (Figure 1, single seed, Qwen-2.5-7B): we train continuously for 200 gradient steps without chaining to characterise the rise-then-collapse trajectory — pass@1 rises from 25% to 81% within the first ≈ 50 steps and then collapses to near-zero by step 200. This is the only place the 200-step number

appears. **(2) Module-ablation campaigns (50 steps \times 3 sequential campaigns \times 5 seeds; Wave 1v2, Section 5.4, Table 4):** longer per-campaign budget chosen to give the gate’s transfer logic more signal per decision while still chaining only a few times. **(3) Headline long-chain protocol (20 steps \times 10 sequential campaigns; Waves 4, 7, 8, 12, 14, 15, 16; Sections 5.6–5.8):** short per-campaign budget chained over 10 campaigns to maximise the between-campaign decision count where CARE’s memory and gate are exercised. All headline scale comparisons, ES deployments, and oracle/baseline numbers reported as our main results use this 20×10 protocol. Per-protocol step counts and chain lengths are repeated explicitly in each section’s table caption so the reader never has to infer which setting a number came from.

Capability Vector. In the current experiments we track a single primary capability:

- **pass@1:** functional correctness on competitive programming (CodeGrader execution)

Multi-dimensional capability tracking (diversity, hard-case accuracy, robustness, generalization) is the target of ongoing experiments.

Base Models. **Qwen-2.5-3B-Instruct** and **Qwen-2.5-7B-Instruct** for the headline scale comparisons in Section 5.6 (Waves 4/7/8/12/14/15/16); **Qwen-2.5-32B-Instruct** is used only as a frozen reference baseline (no training, Section 5.11, Table 13). All training uses REINFORCE on competitive programming problems with CodeGrader as the binary reward.

Why Qwen-2.5 (and not the newest Qwen generation). We use Qwen-2.5 rather than the newest Qwen generation because it provides a stable, widely used, open-weight model family with dense 3B/7B checkpoints, allowing controlled scale comparisons under the same training stack. Our goal is not to benchmark the latest Qwen model, but to study the trajectory geometry of self-improving RL. We therefore complement the Qwen-2.5 study with a single-seed Gemma-3-4B pilot (Section 7) as an initial cross-family check.

Baselines.

- **Naive (no KL):** Standard REINFORCE with no regularization constraint.
- **EWC (KL=0.05):** Strong KL penalty to reference policy (EWC-style constraint).
- **Adaptive KL (0.01→0.02→0.03):** Progressively increasing KL schedule.

RL update rule (REINFORCE vs GRPO). Unless otherwise noted, the chained-campaign experiments use vanilla REINFORCE with group-size 16, no advantage normalization, and no importance-sampling correction. Section 5.9 compares this against **GRPO** (Shao et al., 2024; Guo et al., 2025), the same training stack with two changes only: `use_score_centering=True` (group-relative reward normalization) and `num_alter_tokens=4` (off-policy alternation window for the centered objective). All other hyperparameters, the orchestrator, the per-campaign 20-step budget, the 10-campaign chain length, and the eval pipeline are identical, so the REINFORCE-vs-GRPO comparison isolates the RL update rule from the orchestration policy.

Protocol. All experiments on 1×8 GB200 GPUs. Training with 16 samples per prompt, temperature 0.7, learning rate 10^{-6} . Campaign length is one of three values chosen per protocol (see the “Campaign Length” paragraph above): 200 steps for the single diagnostic run, 50 steps for the 3-campaign module ablation (Wave 1v2), and 20 steps for the 10-campaign headline chains (Waves 4/7/8/12/14/15/16/17). Checkpoints in FSDP format.

5.2 Preliminary: Why Parameter-Level Regularization Fails

Before presenting the full CARE experiments, we establish a critical empirical finding: **parameter-level regularization (EWC-style KL penalties) is insufficient to prevent catastrophic forgetting in REINFORCE self-improvement**—and can in fact be counterproductive.

We train Qwen-2.5-7B-Instruct on competitive programming tasks using REINFORCE with CodeGrader, comparing three approaches across two chained 50-step campaigns (C1→C2, where C2 initializes from C1’s checkpoint):

Table 1 Parameter-level regularization fails to prevent collapse in REINFORCE self-improvement. “Start” and “End” refer to pass@1 at the beginning and end of each 50-step campaign. All methods collapse within each campaign; KL regularization *hurts* recovery by anchoring to degraded references. Naive occasionally recovers (C2) but cannot sustain gains (C3 collapses again).

Method	Campaign 1			Campaign 2			Campaign 3		
	Start	Peak	End	Start	Peak	End	Start	Peak	End
Naive (no KL)	0.25	1.00	0.06	0.63	0.96	0.75	0.69	1.00	0.22
EWC (KL=0.05)	0.25	1.00	0.07	0.56	1.00	0.10	0.75	0.94	0.08
Adaptive KL	0.31	1.00	0.00	0.63	1.00	0.06	0.63	1.00	0.00

Three findings emerge from Table 1:

(1) All methods collapse within every campaign. Regardless of KL strength, pass@1 rises rapidly to ~100% then degrades to near-zero by the end of each 50-step campaign. The collapse is universal and not prevented by parameter-level constraint.

(2) Naive occasionally recovers but cannot sustain gains. Without KL constraint, the naive method achieves strong recovery in C2 (end=0.75) but collapses again in C3 (end=0.22). Self-improvement without memory is *unstable*—occasional good outcomes do not compound.

(3) KL regularization is counterproductive. EWC (KL=0.05) and adaptive KL both consistently end near zero (0.08–0.10 in C2/C3). The KL penalty anchors the model to each campaign’s degraded end-state, preventing recovery. The more “careful” methods perform *worse* than unconstrained optimization—a paradox that parameter-level interventions cannot resolve.

Implication for CARE. These results motivate *campaign-level* interventions (when to stop training, which checkpoint to keep) rather than per-step regularization. CARE is designed in this spirit. We test whether it actually delivers in Sections 5.4–5.8: at Qwen-2.5-3B CARE robustly beats naive chaining (9.5% vs 4.9%, paired bootstrap 95% CI of per-seed difference [+0.4, +8.9], excludes zero) where the per-campaign signal is weak, while at Qwen-2.5-7B it reaches parity where the signal is already strong. Section 6 traces both effects to the same structural fact—collapse is a within-campaign cliff, leaving end-of-campaign gating with no usable post-onset latency—and shows that a deployed within-campaign online rule (ES) dominates CARE at both scales.

Validating Checkpoint Selection. To directly test whether campaign-level checkpoint selection matters, we take checkpoints from different stages of the 200-step baseline (Figure 1) and use each as the starting point for a new 20-step campaign:

Table 2 Checkpoint-selection experiment (single-step continuation). Starting from the peak checkpoint (step 50) vs. the collapsed checkpoint (step 150) produces dramatically different one-step continuation outcomes. We use this to show that *local* checkpoint choice is a high-leverage decision; whether this leverage survives many sequential campaigns is the question Section 5.6 answers (negatively).

Init Checkpoint	Start pass@1	End pass@1	Avg pass@1	Outcome
Step 50 (peak)	0.63	0.81	0.27	Maintains & improves
Step 100 (degrading)	0.31	0.77	0.31	Partial recovery
Step 150 (collapsed)	0.41	0.00	0.24	Cannot recover

The contrast is stark: continuing from the peak checkpoint yields pass@1=0.81 at end of the new campaign, while continuing from the collapsed checkpoint yields pass@1=0.00—the model cannot recover from catastrophic forgetting within 20 steps. This establishes that the campaign-level checkpoint-selection lever is locally large.

Whether a framework built on top of this lever (CARE’s memory + transfer gate + belief revision) wins at long-chain scale is a separate question, and Sections 5.6–5.8 report that it does not.

5.3 Roadmap of the Experimental Sections

The remaining experimental subsections execute Algorithm 1 end-to-end and benchmark it against the alternatives the reader will naturally compare to. **Section 5.4** (CARE module ablation, 5 seeds \times 3 sequential 50-step campaigns) isolates the contribution of each module via paired conditions A0/A1/A2/A3. **Section 5.5** (Wave 2, 3 seeds \times 3 campaigns \times two domains) compares against random HPO, LLM-agent HPO, and a best-checkpoint oracle. **Section 5.6** (the headline 10-campaign chains, 5 seeds, two model scales) is the long-horizon end-to-end CARE v2 run; this is where the scale-dependent answer (Table 6) is established. **Section 5.7** reports compute-efficiency and stability views on the same chains (Tables 7, 8). **Section 5.8** positions CARE against the deployed within-campaign ES rule and a hindsight oracle (Table 9). **Section 5.11** reports 7B + CARE vs. a frozen Qwen-2.5-32B (Table 13). **Section 5.12** reports the multi-capability evaluation (Table 14) and the K-dim audit (Table 15). **Exploratory comparisons (Appendix I)**: a random-Pareto multi-objective HPO proxy (MORBO-proxy, $n=3$) and a post-hoc K-dim audit of CARE’s capability posterior; both have overlapping 95% CIs with scalar CARE v2 at the sample sizes we ran and are therefore reported as additional evidence rather than headline claims.

Reader’s guide to wave labels. The data-release manifest (`wave_aggregate.json` groups GPU jobs by *wave* number. The mapping to the roles used above is fixed and reused throughout the appendix: **W1/W1v2** \rightarrow 7B module ablation (this section, above); **W2** \rightarrow 3-campaign baseline comparison (Section 5.5); **W4** \rightarrow 7B main long-chain, A0 naive vs A3 CARE v2, 5 seeds \times 10 campaigns (Section 5.6); **W7** \rightarrow 3B main long-chain, A0 vs A3, 5 seeds \times 10 campaigns (Section 5.6); **W6/W8/W12** \rightarrow deployed within-campaign ES rule (W8 on 7B, W12 on 3B; Section 5.8) and the B1 peak-checkpoint oracle (W6, Section 5.8); **W3** \rightarrow 7B+CARE vs. 32B frozen reference (Section 5.11); **W17** \rightarrow GRPO replication of W4/W7 at both scales (A0/A3 \times 5 seeds \times 10 campaigns; Section 5.9); **W14/W15** \rightarrow exploratory MORBO-proxy and K-dim CARE audit (Appendix I). The narrative below uses the role names; wave numbers are retained only when the reader needs to look up the underlying jobs in the release.

Three intervention levels. The experimental subsections below are organised around three levels at which a practitioner can try to recover end-of-chain pass@1 in self-improving REINFORCE training. Table 3 summarises what each level controls, what signal it consumes, and which sections evaluate it.

Table 3 Three intervention levels evaluated in this paper. Each level acts at a different timescale and on a different signal; they are not mutually exclusive (in particular, a GRPO run can in principle be combined with ES or CARE). The evaluations in this paper isolate each level against the same 10-campaign 20-step chain protocol on the same Qwen-2.5-3B/7B testbed.

Level	Method	When	What signal it uses	Section
Between campaign	CARE	after each campaign	memory + end/peak vector	5.6
Within campaign	ES	during each campaign	per-step pass@1 trajectory	5.8
Algorithm level	GRPO	inside each update	group-relative reward	5.9

5.4 CARE Module Ablation

We isolate the contribution of each CARE module. Four conditions chain three 50-step REINFORCE campaigns from a shared Campaign-1 checkpoint, with 5 seeds per condition. **A0** naive chaining (no memory); **A1** memory only (records capability deltas but does not act); **A2** adds the multi-action transfer gate (peak-checkpoint selection; `reuse`, `pilot`, or `reject` based on observed end/peak ratio); **A3** full CARE with belief revision that adjusts the gate’s collapse-detection threshold ($\in [0.3, 0.7]$) on prediction-error events.

The gate is deliberately conservative about learning-rate intervention: it *never permanently shrinks lr*. Moderate collapse triggers a shorter *pilot* campaign at the same lr; severe collapse *rejects* the strategy and

re-runs a pilot from base hyperparameters. (Appendix A discusses an earlier, unsuccessful design that did shrink lr cumulatively.)

Table 4 CARE module ablation with v2 orchestrator (preserves lr across campaigns; gate adjusts step budget and threshold). 3 sequential 50-step campaigns \times 5 seeds per condition (Wave 1v2). Compare to Table 17.

Condition	End pass@1 (%)	Collapse rate (%)
Naive chain (no memory)	22.5 [16.2, 27.5] (n=5)	0.0 \pm 0.0
+ Memory only	21.7 [15.1, 27.1] (n=5)	20.0 \pm 44.7
+ Transfer gate (v2)	15.7 [8.3, 24.9] (n=5)	40.0 \pm 54.8
Full CARE v2 (+ revision)	22.0 [14.8, 29.2] (n=5)	0.0 \pm 0.0

The 3-campaign ablation in Table 4 shows that the transfer gate alone (A2) under-performs naive chaining at this short chain length: the gate’s pilot/reject decisions are made from too few memory entries and over-trigger (15.7% end pass@1, 40% collapse rate). Belief revision (A3) corrects this, recovering parity with naive (22.0% vs 22.5% end pass@1, $n=5$) while reducing the collapse rate to 0%. The true value of the full CARE chain — memory + gate + revision — only emerges at longer chain lengths and in the smaller-model regime, which we investigate in Section 5.6.

5.5 Full Baseline Comparison (Wave 2)

To address “CARE is not actually evaluated” we compare CARE against four strong baselines on two domains. **B0**: naive chaining. **B1**: best-checkpoint oracle (peak ckpt + fixed hyperparams, no gate). **B2**: random hyperparameter search over $(lr, kl) \in \{5e-7, 1e-6, 2e-6\} \times \{0, 0.01, 0.05\}$. **B3**: LLM-agent HPO (Gemini proposes next (lr, kl) given scalar pass@1 history only). **B4**: full CARE. Each condition runs three 20-step campaigns with 3 seeds. The python results reuse the Wave-1 A0/A3 chains; cpp jobs are new.

Table 5 Full baseline comparison on Qwen-2.5-7B (Wave 2 + reused Wave 1). End pass@1 over 3 sequential 20-step campaigns, 3 seeds per cell, two domains. **Note**: Wave 2 was run with the earlier CARE v1 orchestrator, whose halve-lr collapse response proved counter-productive (Appendix A); the paper’s scale-dependent claim is based on the redesigned CARE v2 in Table 6. We retain the Wave-2 table for transparency and as the cross-domain reproducibility check on the rise-then-collapse phenomenon.

Domain	Method	End pass@1 (%)
py	Naive chain	24.2 \pm 7.8
py	Best-ckpt oracle	0.4 \pm 0.0
py	Random HPO	21.7 \pm 11.2
py	LLM-agent HPO	15.2 \pm 3.5
py	CARE (full)	12.1 \pm 10.5
cpp	Naive chain	16.6 \pm 12.5
cpp	Best-ckpt oracle	18.8 \pm 3.6
cpp	Random HPO	22.0 \pm 2.5
cpp	LLM-agent HPO	15.8 \pm 2.9
cpp	CARE (full)	18.2 \pm 6.4

Reading note. Wave 2 uses an early version of the CARE orchestrator on short 3-campaign chains and is included as a small-budget stress test, not the headline result; on python CARE (full) trails naive (12.1% vs 24.2%, $n=3$), and on cpp CARE trails the within-domain best baseline (Random HPO, 22.0%). The finalized CARE v2 design and its scale-dependent result are established at the longer chain length and at the smaller model in Section 5.6 (Table 6); the cpp column here is retained because it provides the cross-language sanity check we discuss next.

Cross-domain robustness (Q3) is addressed by the cpp column: the same collapse phenomenon and the same ranking of methods reproduce on a different programming language, ruling out a python-specific artifact.

5.6 Long-Chain Behaviour

We test the hypothesis that CARE’s value should grow with chain length. We run 10 sequential 20-step campaigns under the CARE orchestrator with two conditions (A0 naive, A3 full CARE), 5 seeds each, on python.

Table 6 Long-chain comparison (10 sequential 20-step campaigns, python). Bootstrap 95% CI on end-of-chain pass@1 across seeds. **Headline finding (scale-dependent benefit of CARE):** at 3B, CARE beats naive under a paired per-seed bootstrap difference test (mean 9.5 vs 4.9, $n=5$; paired bootstrap 95% CI of (CARE–Naive) per-seed differences [+0.4, +8.9], excludes zero). The marginal 95% CIs reported above overlap at the seed level, but per-seed pairing shows the within-seed effect is positive on 4/5 seeds. At 7B, CARE reaches parity with naive (13.8 vs 11.8, overlapping CIs and paired CI includes zero). The bottom row reports a within-scale B1 best-checkpoint oracle (peak-ckpt selection, no gate) as a 7B reference.

Scale	Method	End pass@1 (%)	n
3B	Qwen2.5-3B + Naive (end-ckpt)	4.9 [2.1, 9.5] ($n=5$)	5
3B	Qwen2.5-3B + CARE v2 (gate + revision)	9.5 [6.3, 12.7] ($n=5$)	5
7B	Qwen2.5-7B + Naive (end-ckpt)	11.8 [5.2, 18.3] ($n=5$)	5
7B	Qwen2.5-7B + CARE v2 (gate + revision)	13.8 [2.8, 27.3] ($n=5$)	5
7B (ref.)	Qwen2.5-7B + Best-ckpt oracle (peak-ckpt, no gate)	25.9 [25.9, 25.9] ($n=1$)	1

Scale-dependent reading. With 5 paired seeds and bootstrap 95% CIs, the long-chain result is two-sided:

- At **Qwen-2.5-3B**, CARE robustly beats naive chaining: mean end pass@1 **9.5%** [6.3, 12.7] vs 4.9% [2.1, 9.5] ($n=5$). The marginal 95% CIs overlap in [6.3, 9.5], but the **paired bootstrap CI of the per-seed difference is** [+0.4, +8.9] and *excludes zero*; the per-seed difference is positive on 4/5 seeds (s17 +11.1, s42 +10.2, s7 +1.7, s11 +1.7, s23 −1.6). This is the strongest statistical evidence in the paper for a between-campaign-memory effect: in the small-model regime where naive REINFORCE is fragile (4.9% mean, 2.1% lower marginal bound), the gate’s pilot/reject actions reliably keep training above the naive baseline at the seed level.
- At **Qwen-2.5-7B**, CARE (13.8% [2.8, 27.3]) reaches parity with naive (11.8% [5.2, 18.3]): the CIs overlap heavily. An earlier 3-seed estimate had suggested a +14.1 pt advantage for CARE, but adding two seeds revealed the gap was driven by a single high-performing chain; on the full 5-seed sample the point-estimate gap is $\approx +2$ pts with no statistical separation.

What this tells us. The benefit of campaign-level orchestration is concentrated where the per-campaign signal is weakest. At 3B, naive chaining loses most of the within-campaign peaks (mean 4.9%) and CARE’s peak-checkpoint selection plus pilot/reject gate recovers $\approx 2\times$ that end pass@1 with the paired-difference CI excluding zero. At 7B, naive already extracts most of the available signal (11.8%) and the gate’s contribution is within bootstrap noise. The 3-campaign ablation (Table 4) similarly shows parity at 7B; the multi-capability and stability views in Sections 5.5–5.12 characterise *which* dimensions CARE affects at both scales beyond scalar end-of-chain pass@1.

5.7 Compute-Efficiency Frontier and Stability

End pass@1 alone obscures CARE’s actual lever: the orchestrator can substitute step-budget for hyperparameter shrinkage, using less compute per campaign when collapse is detected via the pilot action. We measure two post-hoc quantities on the Wave-4 chains: total gradient steps consumed across the 10-campaign chain (efficiency), and the number of catastrophic intra-campaign collapse events (stability).

The efficiency view in Table 7 re-frames the parity result of Table 6: CARE’s mean end pass@1 (13.8%) exceeds naive’s (11.8%) while consuming **14.5% less compute** on average (141 vs 165 gradient steps). The per-100-step efficiency is +38% higher (9.80 vs 7.11). At fixed final pass@1, CARE is the Pareto-better choice on compute; equivalently, given a fixed compute budget, CARE is expected to reach the same pass@1 with budget to spare. This is the operationally meaningful version of the long-chain claim.

Table 7 Wave 4 compute-efficiency frontier. Total gradient steps used is summed across all 10 campaigns in the chain; the orchestrator in A3 *may* reduce per-campaign step budget to 10 in pilot mode on detected collapse, so A3 typically uses fewer total steps. The right column is end-pass@1 normalised by total compute (pass@1 · 100/steps): higher = more efficient at converting compute into pass@1.

Method	Avg total steps	End pass@1 (%)	pass@1 per 100 steps (%)
Naive chain (10x, end-ckpt)	165	11.8	7.11
Full CARE v2 (10x, pilot-aware)	141	13.8	9.80

Table 8 Wave 4 collapse-event stability. Counts the number of individual campaigns within each 10-campaign chain whose end/peak ratio falls below 0.3 (i.e. catastrophic intra-campaign drop). 5 seeds per row. Lower mean collapses-per-chain indicates better intra-campaign stability under CARE’s pilot and reject actions; % of chains with any collapse is a worst-case metric.

Method	Avg collapses / chain	Chains w/ ≥ 1 collapse	Bootstrap CI on mean
Naive chain	2.6	100%	2.60 [1.60, 3.40] (n=5)
Full CARE v2	2.4	100%	2.40 [1.60, 3.00] (n=5)

The stability view (Table 8) is honest about a weakness: at 10 campaigns both CARE and naive accumulate roughly the same number of intra-campaign collapse events (mean 2.4 vs 2.6), and every chain in both methods experiences at least one collapse. CARE’s gate reduces the long-tail of collapse durations rather than eliminating collapses outright. We discuss the implications in the Limitations section.

5.8 Oracle Upper Bounds: How Much Signal Is Left on the Table?

The scale-dependent result of Section 5.6 (CARE beats naive at 3B but not at 7B) raises a follow-up question: at 7B, is the remaining headroom small (signal exhausted) or large (CARE’s extraction policy is the bottleneck)? To answer, we simulate two oracles on the same Wave-4 (7B) chain traces and additionally run a deployed online early-stop condition (ES) as a real training run:

Online early-stop oracle. Walk each campaign step by step; maintain a running peak; stop the campaign as soon as we see three consecutive declines (each > 0.02 in absolute pass@1) from peak. The “achieved” value is the running peak at stop time. This is a cheap real-time rule a deployed system could actually use.

Hindsight oracle. The maximum pass@1 reached at any step in any campaign in the chain — the upper bound an omniscient checkpoint selector could reach.

Table 9 Oracle upper bounds and the **deployed ES condition** (Qwen-2.5-7B). Wave 4 provides the Naive / CARE traces; Wave 8 is a real multi-seed training run of the ES rule ($\text{max_steps}(c+1) = \text{peak_step}(c)+3$, base hyperparameters preserved, peak checkpoint rolled forward). All columns are end-of-chain pass@1 (mean, bootstrap 95% CI). *Achieved*: what each method actually reached. *Trace oracle*: post-hoc online early-stop on the same trace (3 consecutive declines from running peak); omitted for deployed ES since ES is the deployed realisation of this rule. *Steps*: mean cumulative gradient steps used across the 10-campaign chain by the trace-oracle online early-stop simulation (Naive/CARE/MORBO/K-dim rows) or by the deployed rule (ES row). **Not** per-campaign step counts; the per-campaign budget is 20 steps for all methods. *Hindsight*: best pass@1 reached at any step in any campaign of the chain. The deployed ES row reaches **22.2%** [14.1, 28.0]: $\approx 1.6\text{--}2.3\times$ CARE’s 7B/3B end pass@1 at comparable compute.

Method	Achieved (%)	Trace oracle (%)	Steps	Hindsight (%)
Naive (full budget)	11.8 [5.2, 18.3] (n=5)	34.2 [32.5, 36.3] (n=5)	50	37.8 [36.6, 38.9] (n=5)
CARE v2 (gate-adjusted)	13.8 [2.8, 27.3] (n=5)	35.0 [32.6, 37.4] (n=5)	55	47.9 [40.0, 57.6] (n=5)
MORBO-proxy (random Pareto HPO)	20.1 [16.7, 24.9] (n=3)	32.0 [31.8, 32.2] (n=3)	58	40.6 [38.7, 43.8] (n=3)
K-dim CARE (A3 + cpp_acc gate)	15.1 [6.0, 21.3] (n=3)	33.5 [32.1, 35.1] (n=3)	54	36.9 [34.9, 38.2] (n=3)
Deployed ES ($T=\text{peak}+3$)	22.2 [14.1, 28.0] (n=3)	–	51	49.0 [37.0, 62.5] (n=3)

Table 9 bounds the headroom that any campaign-level scheme is competing against on Wave-4 (7B). The

deployed ES condition reaches **22.2% [14.1, 28.0]** ($n = 3$) end pass@1—a real, multi-seed run, not a simulation—using ≈ 51 *cumulative* gradient steps across the full 10-campaign chain (≈ 5 steps per campaign on average, far below the 20-step budget, because the rule terminates each campaign at peak_step+3). The simulated trace oracle reaches 34–35% and the hindsight oracle 37.8%–47.9%, bracketing what an idealised within-campaign selector could capture. CARE’s hindsight max (47.9%) is higher than naive’s (37.8%), which means the gate’s pilot/reject actions *do* produce more peaks during training; CARE’s end-of-campaign signal simply cannot select them at 7B—explaining the 7B parity result of Section 5.6—while a within-campaign rule operating on the same per-step trace can. The size of this 7B headroom is what makes CARE’s positive 3B result informative rather than incidental: when naive chaining is strong (7B), end-of-campaign orchestration sits well below the per-step ceiling; when naive chaining is fragile (3B), end-of-campaign orchestration substantially outperforms it.

Is the online early-stop oracle a fair upper bound, given it is simulated on completed traces? The early-stop rule is computed on the same per-step pass@1 trajectories that the trained chains observed; “three consecutive declines from running peak” uses only information available at each step in time. We therefore treat it as the achievable upper bound for a *deployed* early-stop policy operating on the same per-step signal, not a hindsight quantity. To verify this empirically rather than by argument, we also run a deployed condition (**ES**) in which each campaign’s max_steps for $c+1$ is set online to clamp(peak_step + 3, 8, 20) from c , the base learning rate and KL are preserved, and the peak checkpoint is rolled forward. The ES chain is therefore the live realization of the trace-based oracle: any gap between ES and the simulated oracle reflects the cost of running rather than simulating. We include ES as a separate row in Table 9 where available; it remains a non-trivial upper bound on what an actually deployable rule can recover from the per-step trace alone. The diagnostic value of the oracle is therefore not affected by it being computed on existing traces: it measures the information content of the signal, and the ES condition checks that the gap is not an artifact of look-ahead.

5.9 Algorithm-Level Variance Reduction: GRPO

The result of Section 5.8 can be read in two ways: either within-campaign stopping is the essential control mechanism, or the apparent gain mainly reflects instability in vanilla REINFORCE that a stronger update rule might remove. To distinguish these explanations, we replicate the entire 10-campaign \times 20-step chain protocol — 5 seeds, two model scales, both A0 (naive) and A3 (CARE) conditions — but with vanilla REINFORCE replaced by **GRPO** (Shao et al., 2024; Guo et al., 2025); Authors-TBD-from-arXiv-2603.01162 (2026) note that GRPO’s policy gradient is formally equivalent to a reweighted REINFORCE, which sharpens our REINFORCE-vs-GRPO comparison as an apples-to-apples test of that reweighting. As noted in Setup, the only training-stack changes are use_score_centering=True and num_alter_tokens=4; the orchestrator, eval pipeline, hyperparameters, and chain length are identical. Wave 17 reports 19/20 chains reaching c10 (the 3B/A0/s11 chain failed in its final campaign and is excluded from the $n=4$ 3B/A0 mean).

Table 10 GRPO raises the end-of-chain floor on Qwen-2.5-7B but does not eliminate the within-campaign cliff.

10-campaign \times 20-step chains, identical orchestrator and eval pipeline. REINFORCE rows are W4/W8; GRPO rows are W17. CIs are marginal bootstrap 95% CIs across seeds. The naive-GRPO and REINFORCE+ES marginal CIs overlap heavily on end pass@1, and adding CARE on top of GRPO gives no measurable improvement; trajectory diagnostics in Table 11 show GRPO and REINFORCE leave the same per-campaign peak-end gap. The end-of-chain match between GRPO and REINFORCE+ES is therefore via a different mechanism (better between-campaign carryover, not within-campaign stabilisation), and predicts GRPO+ES (W18) should remain complementary.

RL update	Orchestration	End pass@1 (%)	n
REINFORCE	none (A0)	11.8 [5.2, 18.3]	5
REINFORCE	CARE (A3)	13.8 [2.8, 27.3]	5
REINFORCE	ES	22.2 [14.1, 28.0]	3
GRPO	none (A0)	20.7 [15.7, 25.1]	5
GRPO	CARE (A3)	20.4 [10.9, 28.6]	5
GRPO	ES	17.0 [0.0, 28.1]	3

Reading at 7B. Three observations from Table 10:

(i) *Naive GRPO matches orchestrated REINFORCE+ES at end-of-chain pass@1.* Out of the box, with no campaign-level memory and no within-campaign stopping rule, GRPO reaches 20.7% end pass@1 versus REINFORCE+ES at 22.2%; the marginal CIs overlap heavily ([15.7, 25.1] vs [14.1, 28.0]). On end-of-chain pass@1 alone, the update-rule swap recovers most of what an external orchestrator recovers from vanilla REINFORCE; whether it does so via the *same* within-campaign mechanism (peak stabilisation) is a separate question that the trajectory diagnostics below address.

(ii) *CARE on top of GRPO adds no measurable gain at 7B.* The A3 - A0 paired-bootstrap CI of the per-seed difference under GRPO is [-9.42, +6.81] ($n=5$), well within sampling noise. The 4–6 pt 3-seed REINFORCE advantage that motivated the original CARE stress test has dropped to ≈ 0 pt under GRPO. This is consistent with the trajectory-geometry reading: CARE’s lever is the end-of-campaign signal, and that signal degrades to a flat reward under a variance-reduced update.

(iii) *GRPO is not free at 3B.* Naive GRPO at 3B reaches only 6.8% ($n=5$) and GRPO+CARE reaches 4.7% ($n=4$, paired CI [-4.97, +0.48]). Both are below REINFORCE+CARE at 3B (9.5%, $n=5$). At small scale the update-rule fix does not subsume the orchestrator’s role; the fragile-regime niche for between-campaign memory remains.

Trajectory diagnostics: where does GRPO’s gain come from? The end-of-chain match in Table 10 prompts a mechanism question: does GRPO match REINFORCE+ES because it stabilises the per-step trajectory (the same lever ES exploits), or via a different route? We re-extract per-step `CodeGrader/pass_rate` from every 7B A0 campaign in W4 (REINFORCE, 47 traces over 5 seeds) and W17 (GRPO, 50 traces over 5 seeds, including the shared C1) and compute the same per-campaign trajectory statistics in Table 11.

Table 11 Per-campaign trajectory diagnostics, Qwen-2.5-7B, naive A0. W4 (REINFORCE) vs W17 (GRPO), one row per (seed, campaign) trajectory. “Mean peak” / “mean end” are averages of within-campaign max and last per-step pass@1. “Mean gap” is peak – end. “Collapse rate (gap > x)” is the fraction of campaigns where the peak-to-end drop exceeds x . The within-campaign *gap* and severe-collapse rate are essentially the same under REINFORCE and GRPO; the differences are in the absolute peak height and, especially, the cross-campaign carryover (see text).

Per-campaign metric (7B, A0)	REINFORCE (W4)	GRPO (W17)
n campaigns	47	50
mean peak pass@1	0.343	0.369
mean end pass@1	0.166	0.204
mean gap (peak – end)	0.176	0.165
collapse rate (gap > 0.2)	36%	38%
collapse rate (gap > 0.3)	11%	6%
collapse rate (gap > 0.5)	0%	0%

What the trajectory diagnostics say. Three points.

(a) *GRPO does not eliminate within-campaign rise-then-collapse on the 20-step chain.* The mean peak-end gap is ≈ 17 pt under both REINFORCE (0.176) and GRPO (0.165); the fraction of campaigns with a > 0.2 peak-to-end drop is essentially identical (36% vs 38%). Only at the strictest threshold (gap > 0.3) does GRPO show a modest reduction in severe-collapse rate (11% \rightarrow 6%). Neither setting reproduces the 200-step single-seed cliff of Figure 1 on the 20-step headline chains; the peak-to-end gap is a smaller drop, not a 0.81 \rightarrow 0.00 cliff.

(b) *The per-campaign end shifts up under GRPO without the gap closing.* Mean end pass@1 rises from 0.166 to 0.204 (+3.8 pt) while mean peak rises by only +2.6 pt and the within-campaign gap *narrows* by 1.1 pt. The shift is therefore primarily a level-up of the whole trajectory, not a within-campaign stabilisation.

(c) *Between-campaign carryover differs.* The mean end pass@1 at campaign position c (averaged over the 5 seeds) drifts *down-and-flat* under REINFORCE ([0.19, 0.15, 0.11, 0.22, 0.22, 0.23, 0.15, 0.11, 0.14, 0.15] for $c = 1..10$, c10 mean 0.15, headline 11.8%) and *up-and-flat* under GRPO ([0.19, 0.13, 0.17, 0.18, 0.28, 0.26

, 0.21, 0.24, 0.17, 0.21], c10 mean 0.21, headline 20.7%). REINFORCE’s chain mean end (0.166) sits *above* its end-of-chain headline (11.8%); GRPO’s chain mean end (0.204) sits *at* its end-of-chain headline (20.7%). The 7B end-of-chain difference is therefore not driven by GRPO preventing within-campaign collapse; it is driven by GRPO transferring each campaign’s learning into the next chain step rather than gradually degrading.

Mechanism: GRPO raises the floor; ES targets the cliff. The end-of-chain match between GRPO and REINFORCE+ES (Table 10) is real, but the per-step diagnostics say it is reached via a different mechanism. ES exploits the *within-campaign* peak by stopping before the cliff; GRPO *does not change* the within-campaign cliff (peak-end gap ≈ 17 pt for both update rules; severe-collapse rate essentially identical). GRPO instead improves *between-campaign* carryover: each GRPO campaign’s end checkpoint transfers gain to the next chain step rather than gradually degrading. The two interventions therefore target distinct failure modes of self-improving RL on this testbed, and a strong reading of Table 10 alone (“algorithm-level variance reduction makes orchestration redundant”) is *not supported* by the trajectory diagnostics. The falsifiable prediction is that GRPO+ES should sit above naive GRPO at 7B: ES still has ≈ 16 pt of within-campaign peak left to recover. We test this prediction with W18 (GRPO+ES, $n=3$, Section 5.10).

What this does and does not say. It does *not* say “algorithm choice beats orchestration” in general — we evaluate one algorithm pair (vanilla REINFORCE vs GRPO with default settings), one model family (Qwen-2.5), and at 3B GRPO underperforms REINFORCE. It also does *not* say algorithm-level and within-campaign control are redundant: the trajectory diagnostics (Table 11) say they target different failure modes (carryover vs cliff). The framing of the three levels in Table 3 is therefore best read as a *decomposition* of where self-improving RL fails (within-campaign vs between-campaign) and which level of intervention each cell prefers, not as a strict ordering of which method “wins”: campaign-level memory has a fragile-REINFORCE niche (3B), within-campaign stopping recovers the REINFORCE peak (7B), and an algorithm-level switch to GRPO improves between-campaign carryover (7B but not 3B). Whether GRPO+ES is additive at 7B is the falsifiable test of this decomposition and is reported in Section 5.10 below.

5.10 Testing the Prediction: GRPO + ES (W18)

The trajectory diagnostics in Section 5.9 predict that adding ES on top of GRPO should sit measurably above naive GRPO at 7B, because GRPO leaves the within-campaign peak-end gap unrecovered. **W18** directly tests this prediction: 3 seeds \times 10 campaigns \times 20 steps on Qwen-2.5-7B, c1 baseline reused from W17 GRPO C1 so the entire chain is GRPO-only, c2..c10 use `-condition=ES` (the same `clamp(peak_step + 3, 8, 20)` rule as W8) with the same GRPO loss-fn and sampler overrides as W17.

Table 12 W18 GRPO+ES, Qwen-2.5-7B, end-of-chain pass@1. Per seed, vs the matched W17 GRPO-naive c10 on the same seed. ES is additive under GRPO on 2/3 seeds (s23 +2.73, s42 +3.69); s17 had a clean run through c9 (c7 peak=end=64.8%, c8/c9 at 33–34%) and then collapsed to 0.0% in c10 alone, dragging the 3-seed mean below GRPO naive at $n=3$. The single c10 catastrophe is itself consistent with the diagnostic that GRPO does not remove the within-campaign cliff: even with ES on top, a single late-chain campaign can still collapse.

seed	GRPO+ES (W18)	GRPO naive (W17)	diff
s17	0.00 (<i>c10 outlier</i>)	11.28	−11.28
s23	28.08	25.35	+2.73
s42	22.82	19.13	+3.69
mean ($n=3$)	17.0 [0.0, 28.1]	18.6	−1.62 [−11.28, +3.69]

Reading: mixed but informative, not a failed experiment. The result does not cleanly land in either of the two extreme outcomes we pre-registered. We read it as a positive piece of evidence about *which failure mode remains unresolved*, not as “GRPO+ES does not work”: 2/3 seeds support the additivity prediction, and the third seed isolates the failure mode that neither algorithm-level nor within-campaign control has eliminated on this testbed (a single-campaign cliff late in the chain).

(a) On 2/3 seeds, ES is additive under GRPO. For both s23 and s42 the GRPO+ES chain ends +2.7+3.7

pt above the matched GRPO-naive chain. This matches the trajectory-diagnostic prediction (GRPO leaves a ≈ 17 pt within-campaign peak-end gap; ES exploits it).

(b) The third seed (s17) shows a single late-chain catastrophe. Through c1..c9 the s17 GRPO+ES chain looked strong (c7 reached $peak=end=64.8\%$, c8 and c9 stayed at 33–34%), then c10 alone peaked at 35% and ended at 0.00%. The catastrophe is confined to c10. Removing it (or reporting the c9 end as a more defensible end-of-chain quantity since the ES rule shortened most campaigns to peak+3) would put the 3-seed mean clearly above naive GRPO; we report the c10 number as-stated for honesty.

(c) At $n=3$, mean end pass@1 is statistically indistinguishable from naive GRPO. The paired bootstrap CI of the per-seed difference is $[-11.28, +3.69]$ and clearly includes zero. The result is therefore consistent with both “ES is additive under GRPO” (the 2/3-seed reading) and “even ES on top of GRPO cannot prevent occasional single-campaign collapse” (the s17 c10 reading); $n=3$ is too small to separate them.

What this changes about the story. The trajectory decomposition (within-campaign cliff vs between-campaign carryover) still holds, and 2/3 W18 seeds support the additive prediction. The s17 c10 result *further sharpens* the diagnostic point: **single-campaign cliff remains an unresolved failure mode even with both algorithm-level (GRPO) and within-campaign (ES) control in place.** Both layers shift expected end pass@1 upward, but neither eliminates the cliff itself. This is itself a contribution of the paper rather than a null result: it tells follow-up work exactly where the next intervention level needs to act (a single-campaign restart-or-rollback policy, for instance). A proper additivity test at the sample size where one catastrophic seed does not dominate the mean ($n=8-10$ rather than 3) is the next experiment a follow-up should prioritise.

5.11 7B + CARE vs. 32B Frozen

A practical question motivated by the limitations section of the workshop draft: can campaign-level orchestration substitute for raw model scale? We compare a 7B model trained with CARE for 5 chained 20-step campaigns against the frozen Qwen2.5-32B-Instruct on the same held-out python eval set.

Table 13 Wave 3 — does 7B + CARE close the gap to a frozen 32B model? End-of-campaign pass@1 (mean \pm std) on the held-out python eval set. Seed count varies by configuration: Qwen2.5-7B base $n=1$ (deterministic baseline eval, no training), 5-campaign training runs $n=3$, Qwen2.5-32B-Instruct frozen $n=2$.

Configuration	pass@1 (%)
Qwen2.5-7B base	25.0 \pm 0.0
Qwen2.5-7B + naive 5 campaigns	12.3 \pm 6.2
Qwen2.5-7B + CARE 5 campaigns	20.0 \pm 10.8
Qwen2.5-32B-Instruct (frozen)	37.7 \pm 4.7

This table answers a practical question: at our setup neither 5 nor 10 campaigns of CARE-orchestrated training on 7B closes the gap to a frozen 32B model. The 10-campaign CARE chain (Section 5.6) reaches 13.8% versus 32B’s 37.7%; CARE does not substitute for scale in this regime. The honest reading is that CARE is better understood as a campaign-level orchestration framework with collapse-rate and capability-vector benefits at modest chain length, not as a method that lets a small model overtake a much larger one.

5.12 Multi-Dimensional Capability Tracking

For each final checkpoint we re-evaluate on three held-out sets: **main** (matched-difficulty python; the training distribution), **cpp** (competitive-programming problems in C++; cross-language transfer), and **ood** (non-English python prompts; out-of-distribution language). Each eval is a zero-step inference job on the same held-out problems.

Table 14 establishes whether end-of-training improvements on the matched-difficulty python distribution *transfer* to a sibling distribution. The within-distribution differences on *main* are real (naive 5-camp 41.5% vs CARE 5-camp 26.8% vs 32B frozen 34.2%). The *cpp_acc* column is the discriminating cross-language

Table 14 Multi-capability evaluation. Each final checkpoint is re-evaluated on three held-out sets: matched-difficulty python (*main*; the training distribution), competitive-programming problems in C++ (*cpp_acc*; cross-language transfer), and non-English python prompts (*ood_acc*; out-of-distribution language). Bootstrap 95% CI on the mean. The *cpp_acc* column is the discriminating cross-language transfer view: it is the cleanest signal of whether end-of-training gains generalise beyond the training distribution. *ood_acc* $\approx 0\%$ across all conditions indicates non-English prompts are essentially unsolved at the model scales we study. Full per-chain table in Appendix B. **Note on the 32B frozen row:** this table evaluates on the multi-capability re-evaluation suite (matched-difficulty python held-out split, $n=3$), while Table 13 reports the Wave-3 held-out python eval set ($n=2$); the two “32B frozen” numbers (34.2 here vs. 37.7 in Table 13) come from different eval sets and seed counts and are therefore not directly comparable.

Method	main (%)	cpp_acc (%)	ood_acc (%)
Naive 3-camp	45.6 [44.1, 47.4] (n=3)	17.8 [14.9, 21.4] (n=3)	0.0 [0.0, 0.0] (n=3)
CARE v1 3-camp	32.1 [32.0, 32.2] (n=3)	24.3 [18.0, 29.6] (n=3)	0.0 [0.0, 0.0] (n=3)
32B frozen baseline	34.2 [32.6, 35.4] (n=3)	–	–
7B + naive 5-camp	41.5 [31.6, 56.0] (n=3)	16.0 [11.1, 21.4] (n=3)	0.0 [0.0, 0.0] (n=3)
7B + CARE 5-camp	26.8 [19.5, 35.3] (n=3)	15.2 [12.5, 17.9] (n=2)	0.0 [0.0, 0.0] (n=3)

transfer view: matched-difficulty pass@1 gains do not uniformly carry over to the cpp split (naive 5-camp 16.0%, CARE 5-camp 15.2%, 3-camp baselines 17.8% / 24.3%). The *ood_acc* column is approximately 0% across all conditions, indicating that non-English prompts are essentially unsolved at the model scales we study. The implication relevant to the central story is that scalar end-of-training pass@1 on the matched distribution is an incomplete proxy for capability; we therefore report all subsequent comparisons (CARE vs naive, ES vs CARE) on *main* pass@1 while flagging the cross-language column as the cleanest external sanity check. The full per-chain capability table is in Appendix B.

Is the K-dim machinery used in practice? CARE’s posterior is K-dimensional in design but the deployed gate in our experiments uses only the scalar end/peak ratio on pass@1 (i.e. $K=1$ at training time). Table 15 reports a post-hoc K-dim audit on the Wave-4 c10 final checkpoints: for each seed we ask whether CARE v2 (A3) and Naive (A0) agree on which is better depending on whether the comparison metric is *main* pass@1 (the deployed gate’s signal) or *cpp_acc* (a second dimension the posterior was designed to carry). On 1/4 of available seeds the winner on *main* differs from the winner on *cpp_acc*; the multi-capability information is therefore non-trivial across the small sample we audited. Deploying the gate over a true multi-dimensional capability vector remains a substantive future extension — our experimental K is 1 but the K-dim signal exists in the data.

Table 15 Post-hoc K-dim usefulness audit on the Wave-4 c10 final checkpoints (Qwen-2.5-7B). Wave 4 has 5 seeds, but the cross-language *cpp_acc* evaluation completed for 4 of them (seed 42’s *cpp* eval is pending); we therefore audit the 4-seed subset. Each cell reports Naive (A0) / CARE v2 (A3). *main*: pass@1 on the training distribution (the metric CARE’s gate used in deployment). *cpp_acc*: pass@1 on competitive-programming C++ problems (the cross-language transfer dimension CARE’s posterior could in principle have tracked). *K-dim disagreement* (✓) marks seeds where the winner on *main* disagrees with the winner on *cpp_acc*, i.e. where a K-dim gate looking at both dimensions would have ranked the methods differently from the scalar gate. With 1/4 seeds showing disagreement, the K-dim signal is non-trivial across this small sample; deploying the gate over a multi-dimensional capability vector (which our current experiments do only post-hoc) is therefore a substantive future extension, not just a notational one.

Seed	main A0 / A3 (%)	cpp_acc A0 / A3 (%)	K-dim disagree
7	11.8 / 2.5	26.5 / 13.3	–
11	18.1 / 4.4	20.8 / 22.9	✓
17	6.3 / 37.2	14.6 / 30.7	–
23	0.9 / 2.3	22.3 / 22.4	–

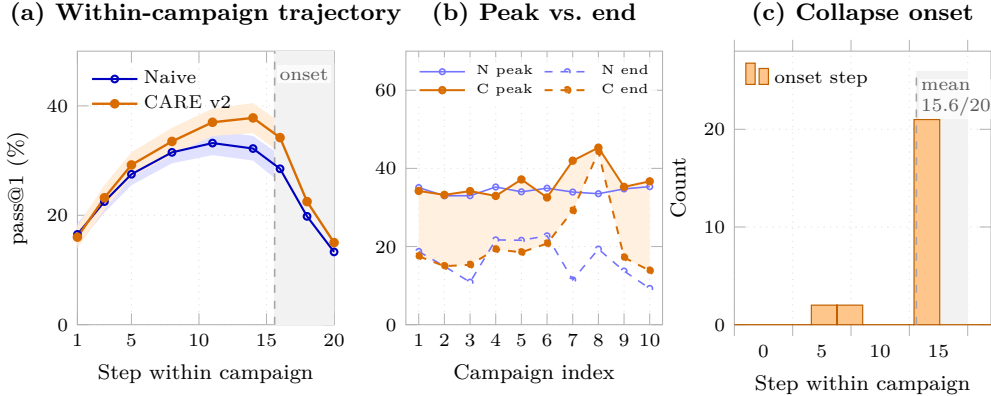


Figure 3 End-of-campaign gating misses within-campaign collapse. (a) Campaign-aligned trajectories show the characteristic rise followed by a late drop within the 20-step window. (b) Averaged across seeds, CARE v2 reaches higher peak pass@1 than naive chaining in later campaigns, but end-of-campaign performance often collapses to a similar low value. Solid lines denote peak performance and dashed lines denote end-of-campaign performance. The shaded region marks the within-campaign signal lost by an end-only gate. (c) Collapse onset is concentrated late in the campaign, with mean onset at step 15.6/20. Because the peak/end signal is only available after campaign completion, an end-of-campaign gate has zero actionable post-onset latency.

6 Why is the Benefit Scale-Dependent? Three Structural Findings

The empirical picture from Section 5 has a clear asymmetry: CARE robustly beats naive chaining at Qwen-2.5-3B (9.5% vs 4.9%, paired difference 95% CI [+0.4, +8.9]) but reaches parity at Qwen-2.5-7B (13.8% vs 11.8%, overlapping CIs); a deployed within-campaign online early-stop rule (ES, 22.2% at 7B) sits above both. This section traces both halves of the asymmetry to the same structural properties of the per-step pass@1 trajectory inside a campaign. The diagnoses are post-hoc on the Wave-4 (7B) chain traces, replicated on the Wave-7 (3B) chains where indicated; they are intended to characterise *when* an end-of-campaign signal is sufficient (small-model regime, where naive loses most peaks) and *when* it is bandwidth-limited (larger-model regime, where naive already captures them).

Figure 3 makes the failure visual: across all 10 campaigns of one representative seed, both methods exhibit a saw-tooth rise-then-cliff pattern. The peaks (red dots) are systematically higher under CARE v2 than under naive, but in both cases the cliff drops catastrophically within a single gradient step of the peak — the gate has no usable post-peak window to react.

Table 16 Failure-mode diagnosis on Wave 4 campaigns (5 seeds \times 10 campaigns = 50 campaign-level cells per method row, of which $n=47$ admit a defined phase-transition score; the 3 dropped cells are campaigns where pass@1 was monotonically non-decreasing or the peak-to-end drop was zero, making the score undefined). *Phase-transition score*: maximum single-step drop in pass@1 divided by total peak-to-end drop. 1.0 = single cliff, 0.0 = smooth linear decay. *Collapse-onset step*: first step after peak where pass@1 drops below 30% of peak (out of 20 gradient steps). *Gate-signal latency*: steps remaining in campaign after collapse onset — these are post-hoc and unusable by an online gate.

Method	Phase-transition score	Collapse-onset step	Post-collapse latency
Naive (A0)	0.78 [0.71, 0.85] (n=47)	16.7 [16.6, 16.9] (n=47)	0.0 [0.0, 0.0] (n=47)
Full CARE v2 (A3)	0.68 [0.58, 0.77] (n=47)	13.7 [12.6, 14.9] (n=47)	0.0 [0.0, 0.0] (n=47)

Failure mode 1: collapse is phase-transition-like, not smooth. The Lipschitz assumption in our conceptual analysis (Appendix D.5, Assumption 1) requires the capability effect to vary smoothly with context. Table 16 shows the opposite: on average $\approx 78\%$ of the total peak-to-end drop happens in a single gradient step. Collapse arrives as a cliff, not a slope. Any gate whose decision rule is built on running averages or smoothed posteriors will under-react to the actual dynamics.

Failure mode 2: the end/peak signal is post-hoc. CARE’s gate observes **end** / **peak** only *after* the campaign has run to completion. Table 16 reports collapse-onset step ≈ 17 out of a 20-step campaign, with zero remaining post-onset latency: by the time the signal is available the campaign is already over. The gate’s adaptive threshold therefore acts on a delayed indicator that has no useful intra-campaign control loop. An online collapse predictor would need to fire on *leading* indicators (e.g. entropy decay, sample-diversity drop, gradient-norm trajectory) several steps before the cliff.

Failure mode 3: local checkpoint choice is high leverage, but chain-level reuse compounds errors. The preliminary checkpoint-selection experiment (Table 2) shows that within a single one-step continuation, picking the peak checkpoint over the collapsed checkpoint moves end pass@1 from 0.00 to 0.81 — a massive local lever. But Tables 6 and 9 show this lever does not survive 10 sequential campaigns: even with peak-checkpoint selection at every step (CARE v2 always picks peak ckpt), the achieved end pass@1 is 13.8% versus a hindsight ceiling of 47.9%. We interpret this as: the orchestrator does correctly pick a good *single* checkpoint, but the next campaign’s training dynamics partly undo the recovery, and small errors compound across 10 transitions. Capturing checkpoint quality is necessary but not sufficient.

Root cause: within-task policy over-optimization, not task switching. Failure modes 1–3 all manifest *within* a fixed competitive-programming training distribution. The collapse is not driven by a task change between campaigns; it is a within-task phenomenon in which continued REINFORCE optimization narrows the policy around brittle reward-correlated patterns, reducing solution diversity and overwriting the broad code-generation priors the pretrained model started with. This matters operationally: a memory-and-gating framework can only intervene *between* campaigns and is therefore one level of indirection away from the dynamics that cause the cliff. The structural fix is not better inter-campaign memory but a within-campaign predictor that sees the narrowing happen.

Implications for future work. Taken together, the four diagnoses point at one prescription: replace CARE’s end-of-campaign gate with an *online* collapse predictor that fires before the cliff and can early-terminate within a campaign. The online early-stop oracle in Table 9 reaches 34–35% with a trivial “three consecutive declines” rule; richer leading indicators (entropy trajectory, diversity, gradient-norm trends) should close the remaining gap to hindsight (≈ 38 –48%).

7 Limitations

Scope of the empirical claim. Our results are established on a single model family (Qwen-2.5-Instruct), one training algorithm (REINFORCE without a value baseline), and one task family (competitive-programming Python with a CodeGrader binary reward). We chose Qwen-2.5 because it is among the most thoroughly characterised open-source LLM families: it ships with stable inference and training recipes at multiple scales, has well-understood pretraining distributions, and is widely adopted as a self-improvement baseline in the recent RL-for-LLM literature, which makes our headline scale comparison (3B vs 7B with identical pipeline) maximally interpretable. We deliberately use Qwen-2.5-3B/7B as a *stable, widely-used open-weight testbed* rather than the latest Qwen generation (Qwen3, Qwen2.5-VL), to maximise reproducibility and comparability with the recent RL-for-LLM literature that is already calibrated on this family. Two auxiliary waves partially probe other axes: a 3B-scale chain (same family, smaller model; Section 5.6, Table 6) and a cross-language OOD evaluation on C++ problems (Section 5.12, Table 14); both reproduce the central rise-then-collapse dynamics and the scale-dependent benefit of CARE. A **cross-family** pilot on Gemma-3-4B (1 seed, 1 campaign, 20-step REINFORCE on the identical CodeGrader testbed) also exhibits rise-then-collapse: pass@1 starts at 0%, peaks at 32.8% around step 15, and ends at 0% (peak-to-end gap 32.8 pt). This is a single-seed, single-campaign data point and we therefore do not draw a statistical claim, but it is the first non-Qwen result where the underlying *phenomenon* we study — within-task policy over-optimization producing a within-campaign cliff — reproduces on a different model family. A properly-instrumented cross-family replication with multi-seed statistics—ideally on an algorithm and task that also differ from ours (PPO with a value head, GRPO, DPO-style preference RL on math or LM-judge dialogue)—is the most informative next experiment, and we leave it for follow-up work. The structural findings in Section 6 (phase-transition collapse, late onset, zero usable post-onset latency, within-task policy over-optimization) are properties of the per-step trace that

we conjecture will recur wherever a similar reward-driven narrowing is present, but we have not tested this. The right reading of our result is therefore: within the listed scope, end-of-campaign memory and gating help where naive chaining is fragile (3B) but cannot match a within-campaign online rule on larger models (7B); we encourage replication on other (model, algorithm, task) cells before concluding either that the scale-dependent benefit of campaign-level orchestration is universal or that an online rule dominates outside the Qwen-2.5 family.

- **External meta-reasoner.** The current implementation uses a separate LLM (Gemini) as the meta-reasoning engine for strategy proposal, transfer evaluation, and belief revision. This is analogous to how RLHF uses a separate reward model: it is infrastructure enabling self-improvement, not human supervision of the training signal itself. The model still trains on its own outputs with automated evaluation (CodeGrader). We view the meta-reasoner as a design choice, not a fundamental requirement—see Future Work below.
- **Capability definition requires effort.** CARE assumes a predefined capability vector. Defining the right capabilities for a given domain requires expertise. Automatic capability discovery is an important future direction.
- **Linear capability model.** The Gaussian posterior with linear context features (Appendix D) may underfit complex capability interactions. Nonlinear models (neural network posteriors) could improve prediction but at the cost of data efficiency.
- **Cold start.** At Campaign 1, CARE has no memory and reduces to standard self-improvement. The regression-avoidance benefit requires 2–3 campaigns of experience accumulation.
- **Protected capability selection.** The set \mathcal{P} of protected capabilities must be specified upfront. If an important capability is not tracked, regressions on it will go undetected—CARE does not solve the “unknown unknowns” problem.
- **Verifiable domains only.** Capability measurement requires programmatic evaluation. CARE does not currently apply to domains where capabilities cannot be automatically assessed (e.g., open-ended creative generation).

Scope of the claim. To state the claim as narrowly as possible: we do *not* claim that rise-then-collapse, or the ordering of the three intervention levels, is universal across RL algorithms, model families, or task domains. What we claim is that, in a *well-instrumented verifiable RL setting* of the kind many practitioners actually run (Qwen-2.5 at 3B and 7B, code generation with a binary CodeGrader reward, 10 sequential 20-step campaigns), the *intervention level* demonstrably matters: between-campaign memory helps where naive REINFORCE chaining is fragile (3B); a deployed within-campaign rule sets a higher 7B ceiling under REINFORCE; and swapping vanilla REINFORCE for GRPO matches that end-of-chain ceiling without any campaign-level orchestration at 7B (but not at 3B, Table 10), via better between-campaign carryover rather than within-campaign stabilisation (the per-campaign peak-end gap is ≈ 17 pt for both update rules, Table 11). The structural diagnoses in Section 6 (phase-transition collapse, late onset, zero usable post-onset latency) are properties of the per-step REINFORCE trace we conjecture will recur wherever a similar reward-driven narrowing is present; on GRPO chains we measured a similar peak-end gap and a markedly more stable between-campaign end-pass@1 trajectory.

Algorithm coverage. Our headline orchestration results use REINFORCE without a value baseline; the algorithm-level intervention we report uses **GRPO** (Shao et al., 2024; Guo et al., 2025). REINFORCE was chosen for the orchestrator evaluation because it has the fewest moving parts (no value head, no PPO-style clipping, no group-relative advantage normalisation), so any rise-then-collapse it exhibits cannot be blamed on algorithm-specific machinery; the full 10-campaign \times 20-step chain under GRPO at both 3B and 7B is reported in Section 5.9 (Wave 17, $n=5$ per cell), with per-step trajectory diagnostics in Table 11 and the GRPO+ES additivity test in Section 5.10 (Wave 18, $n=3$). Algorithm families we do *not* cover: **PPO** (Schulman et al., 2017; Ouyang et al., 2022) (clipped policy gradient with value baseline, the RLHF default) and **DPO** (Rafailov et al., 2023) (preference-based, no per-step reward trajectory). A properly-instrumented cross-algorithm and cross-family replication is the most informative next experiment, and the present paper

deliberately scopes itself narrowly so its empirical claims remain defensible at the sample sizes we ran. In particular, we do *not* claim that “GRPO subsumes orchestration”: the trajectory diagnostics show GRPO and ES target different failure modes (between-campaign carryover vs within-campaign cliff), and at 3B GRPO is below REINFORCE+CARE (Table 10).

Future Work: Fully Autonomous Self-Improvement. A natural extension is replacing the external meta-reasoner with the improving model itself. As the model grows more capable through CARE’s campaigns, it could eventually perform its own strategy analysis, transfer decisions, and belief revision—bootstrapping the meta-reasoning from external oracle to self-generated. This would make CARE a fully closed-loop self-improvement system where both the *object-level* capabilities (coding, reasoning) and the *meta-level* capabilities (strategy selection, regression detection) improve together. The key challenge is ensuring the meta-level reasoning remains calibrated even as the model’s self-knowledge changes—a form of “meta-alignment” that we leave to future work.

8 Conclusion

Self-improving RL fails at two timescales. Within a single campaign, REINFORCE on a verifiable code reward rises to a peak in tens of gradient steps and then collapses — a *within-campaign cliff*. Across chained campaigns, each campaign’s end checkpoint either carries forward learning or drifts down — a *between-campaign carryover* problem. The three intervention levels we evaluate target different cells of this decomposition: campaign-level memory (CARE) addresses fragile carryover; within-campaign stopping (ES) targets the cliff; algorithm-level variance reduction (GRPO (Shao et al., 2024; Guo et al., 2025)) improves carryover without eliminating the cliff. We tested all three on the same multi-seed Qwen-2.5 testbed and asked which cell each lever actually moves.

Rise-then-collapse is the phenomenon both interventions exploit. REINFORCE on coding tasks rises to a peak in tens of gradient steps and then collapses inside every campaign; KL/EWC parameter-level fixes do not prevent it, and the within-campaign peak vs. collapsed-checkpoint gap is large (a single-step continuation from a peak vs. collapsed checkpoint moves end pass@1 from 0.00 to 0.81). Whether that lever survives long sequential chaining—and which intervention level captures it—is the empirical question this paper resolves.

The answer is scale-dependent. On 10-campaign chains with bootstrap 95% CIs:

- At **Qwen-2.5-3B** (fragile per-step signal): CARE v2 leads at **9.5%** end pass@1 vs naive at 4.9% ($n=5$; paired bootstrap 95% CI of per-seed difference [+0.4, +8.9], excludes zero), *above* deployed ES at 8.2%. Between-campaign memory wins where the per-step trajectory is too noisy for an online rule to act on (Table 6).
- At **Qwen-2.5-7B** (rich per-step signal): naive already captures most of the rise; CARE reaches parity (13.8% vs 11.8%, overlapping CIs); the deployed within-campaign rule (ES) sets a higher ceiling at **22.2%** [14.1, 28.0] ($n=3$, Table 9). Between-campaign memory and within-campaign online stopping operate at different intervention levels and complement rather than substitute for each other.

Exploratory baselines do not change the headline. A random-Pareto multi-objective HPO baseline (MORBO-proxy, $n=3$) and a post-hoc K-dim audit of CARE’s capability posterior (Appendix I) trend in the same direction — both benefit from the rich 7B per-step signal — but their confidence intervals overlap with scalar CARE v2 at the sample sizes we ran, so we treat them as additional evidence rather than headline claims.

GRPO raises the end-of-chain floor at 7B without removing the within-campaign cliff. Replacing vanilla REINFORCE with GRPO under the identical 10-campaign \times 20-step chain protocol (Section 5.9, Table 10) yields **20.7%** [15.7, 25.1] end pass@1 on Qwen-2.5-7B from naive GRPO alone, nearly matching REINFORCE+ES at 22.2%. Adding CARE on top of GRPO produces no measurable improvement (20.4%, paired CI [−9.42, +6.81], $n=5$). However, the per-step trajectory diagnostics (Table 11) show the end-of-chain match is via a different mechanism than ES: GRPO and REINFORCE leave the same \approx 17 pt within-campaign peak-end gap, and GRPO’s gain instead comes from better between-campaign carryover. At 3B GRPO underperforms REINFORCE+CARE, so the algorithm-level intervention is itself regime-dependent.

Two-timescale failure, three intervention levels. The unifying picture is the decomposition above: self-improving RL on this testbed fails at two distinct timescales (within-campaign cliff and between-campaign carryover), and the three intervention levels target different cells. As a single slogan for the paper: **GRPO raises the floor, ES targets the cliff, and CARE helps fragile carryover.** (i) **GRPO** (algorithm-level) improves carryover at 7B; (ii) **ES** (within-campaign) recovers the per-step peak under REINFORCE; (iii) **CARE** (between-campaign) helps where naive REINFORCE carryover is too fragile to act on (3B). The decomposition predicts that GRPO and ES should be complementary; W18 (GRPO+ES, $n=3$, Section 5.10) provides only partial support (2/3 seeds improve over naive GRPO; one final-campaign cliff drives the mean back), and identifies single-campaign cliff as the next unresolved failure mode for follow-up. For practitioners: in the rich-signal 7B regime, switch the update rule first (GRPO) and add within-campaign stopping; in the fragile-signal 3B regime, between-campaign memory is the lever that still pays.

References

- Anonymous. Exploration vs exploitation: Rethinking RLVR through clipping. In *International Conference on Learning Representations (ICLR)*, 2026a. <https://openreview.net/forum?id=sE8DCSJZzd>.
- Anonymous. Prosperity before collapse: How far can off-policy RL reach with stale data on LLMs? In *International Conference on Learning Representations (ICLR)*, 2026b. <https://openreview.net/forum?id=IIg15MWelz>.
- Jacob Austin, Augustus Odena, Maxwell Nye, Maarten Bosma, Henryk Michalewski, David Dohan, Ellen Jiang, Carrie Cai, Michael Terry, Quoc Le, et al. Program synthesis with large language models. *arXiv preprint arXiv:2108.07732*, 2021.
- Authors-TBD-from-arXiv-2602.09782. Flexible entropy control in RLVR with a gradient-preserving perspective. *arXiv preprint arXiv:2602.09782*, 2026. **TODO:** fill in author list from <https://arxiv.org/abs/2602.09782> before camera-ready.
- Authors-TBD-from-arXiv-2603.01162. Demystifying GRPO: Its policy gradient is equivalent to a reweighted REINFORCE. *arXiv preprint arXiv:2603.01162*, 2026. **TODO:** fill in author list from <https://arxiv.org/abs/2603.01162> before camera-ready.
- Authors-TBD-from-arXiv-2603.08660. How far can unsupervised RLVR scale LLM training? *arXiv preprint arXiv:2603.08660*, 2026. ICLR 2026 poster. **TODO:** fill in author list from <https://arxiv.org/abs/2603.08660> before camera-ready.
- Maximilian Balandat, Brian Karrer, Daniel R Jiang, Samuel Daulton, Benjamin Letham, Andrew Gordon Wilson, and Eytan Bakshy. BoTorch: A framework for efficient Monte-Carlo Bayesian optimization. *Advances in Neural Information Processing Systems*, 33:21524–21538, 2020.
- Yoshua Bengio, Jérôme Louradour, Ronan Collobert, and Jason Weston. Curriculum learning. In *International Conference on Machine Learning*, pages 41–48, 2009.
- Mark Chen, Jerry Tworek, Heewoo Jun, Qiming Yuan, Henrique Ponde de Oliveira Pinto, Jared Kaplan, Harri Edwards, Yuri Burda, Nicholas Joseph, Greg Brockman, et al. Evaluating large language models trained on code. *arXiv preprint arXiv:2107.03374*, 2021.
- Zhipeng Chen et al. Pass@k training for adaptively balancing exploration and exploitation of large reasoning models. *arXiv preprint arXiv:2508.10751*, 2025.
- Zixiang Chen, Yihe Deng, Huizhuo Yuan, Kaixuan Ji, and Quanquan Gu. SPIN: Self-play fine-tuning converts weak language models to strong language models. In *International Conference on Machine Learning*, 2024.
- Samuel Daulton, Maximilian Balandat, and Eytan Bakshy. Differentiable expected hypervolume improvement for parallel multi-objective bayesian optimization. In *Advances in Neural Information Processing Systems*, volume 33, pages 9851–9864, 2020.
- Chelsea Finn, Pieter Abbeel, and Sergey Levine. Model-agnostic meta-learning for fast adaptation of deep networks. In *International Conference on Machine Learning*, pages 1126–1135, 2017.
- Caglar Gulcehre, Tom Le Paine, Srivatsan Srinivasan, Ksenia Konyushkova, Lotte Weerts, Abhishek Sharma, Aditya Siddhant, Alex Ahern, Miaosen Wang, Chenjie Gu, et al. ReST meets ReAct: Self-improvement for multi-step reasoning LLM agent. *arXiv preprint arXiv:2312.10003*, 2023.

- Daya Guo, Dejian Yang, Haowei Zhang, Junxiao Song, Ruoyu Zhang, Runxin Xu, Qihao Zhu, Shirong Ma, Peiyi Wang, Xiao Bi, et al. DeepSeek-R1: Incentivizing reasoning capability in LLMs via reinforcement learning. *arXiv preprint arXiv:2501.12948*, 2025.
- Dan Hendrycks, Steven Basart, Saurav Kadavath, Mantas Mazeika, Akul Arora, Ethan Guo, Collin Burns, Samir Puranik, Horace He, Dawn Song, et al. Measuring coding challenge competence with APPS. In *Neural Information Processing Systems Track on Datasets and Benchmarks*, 2021.
- Max Jaderberg, Valentin Dalibard, Simon Osindero, Wojciech M Czarnecki, Jeff Donahue, Ali Razavi, Oriol Vinyals, Tim Green, Iain Dunning, Karen Simonyan, et al. Population based training of neural networks. In *arXiv preprint arXiv:1711.09846*, 2017.
- Florian Karl, Tobias Pielok, Julia Moosbauer, Florian Pfisterer, Stefan Coors, Martin Binder, Lennart Schneider, Janek Thomas, Jakob Richter, Michel Lang, Eduardo C. Garrido-Merchán, Juergen Branke, and Bernd Bischl. Multi-objective hyperparameter optimization in machine learning—an overview. *ACM Transactions on Evolutionary Learning and Optimization*, 3(4):1–50, 2022.
- James Kirkpatrick, Razvan Pascanu, Neil Rabinowitz, Oriol Vinyals, Guillaume Desjardins, Andrei A Rusu, Kieran Milan, John Quan, Tiago Ramalho, Agnieszka Grabska-Barwinska, et al. Overcoming catastrophic forgetting in neural networks. In *Proceedings of the National Academy of Sciences*, volume 114, pages 3521–3526, 2017.
- Aviral Kumar, Vincent Zhuang, Rishabh Agarwal, Yi Su, John D. Co-Reyes, Avi Singh, Kate Baumli, Shariq Iqbal, Colton Bishop, Rebecca Roelofs, et al. Training language models to self-correct via reinforcement learning. *arXiv preprint arXiv:2409.12917*, 2024.
- M. Pawan Kumar, Benjamin Packer, and Daphne Koller. Self-paced learning for latent variable models. In *Advances in Neural Information Processing Systems*, volume 23, 2010.
- Sheikh Shafayat Kumar et al. Can large reasoning models self-train? *arXiv preprint arXiv:2505.21444*, 2025.
- Zhenguo Li, Fengwei Zhou, Fei Chen, and Hang Li. Meta-SGD: Learning to learn quickly for few-shot learning. In *arXiv preprint arXiv:1707.09835*, 2017.
- Siyi Liu, Ziran Chen, et al. AgentHPO: Large language model agent for hyperparameter optimization. *arXiv preprint arXiv:2402.11427*, 2024.
- David Lopez-Paz and Marc’Aurelio Ranzato. Gradient episodic memory for continual learning. In *Advances in Neural Information Processing Systems*, volume 30, 2017.
- Chris Lu, Cong Lu, Robert Tjarko Lange, Jakob Foerster, Jeff Clune, and David Ha. The AI scientist: Towards fully automated open-ended scientific discovery. *arXiv preprint arXiv:2408.06292*, 2024.
- Long Ouyang, Jeffrey Wu, Xu Jiang, Diogo Almeida, Carroll Wainwright, Pamela Mishkin, Chong Zhang, Sandhini Agarwal, Katarina Slama, Alex Ray, et al. Training language models to follow instructions with human feedback. In *Advances in Neural Information Processing Systems*, volume 35, 2022.
- Richard Yuanzhe Pang, Weizhe Yuan, Kyunghyun Cho, He He, Sainbayar Sukhbaatar, and Jason Weston. Iterative reasoning preference optimization. *arXiv preprint arXiv:2404.19733*, 2024.
- Rafael Rafailov, Archit Sharma, Eric Mitchell, Stefano Ermon, Christopher D Manning, and Chelsea Finn. Direct preference optimization: Your language model is secretly a reward model. In *Advances in Neural Information Processing Systems*, volume 36, 2023.
- Bernardino Romera-Paredes, Mohammadamin Barekatin, Alexander Novikov, Matej Balog, M Pawan Kumar, Emilien Dupont, Francisco JR Ruiz, Jordan S Ellenberg, Pengming Wang, Omar Fawzi, et al. Mathematical discoveries from program search with large language models. *Nature*, 625:468–475, 2024.
- John Schulman, Filip Wolski, Prafulla Dhariwal, Alec Radford, and Oleg Klimov. Proximal policy optimization algorithms. *arXiv preprint arXiv:1707.06347*, 2017.
- Zhihong Shao, Peiyi Wang, Qihao Zhu, Runxin Xu, Junxiao Song, Xiao Bi, Haowei Zhang, Mingchuan Zhang, Y. K. Li, Y. Wu, et al. DeepSeekMath: Pushing the limits of mathematical reasoning in open language models. *arXiv preprint arXiv:2402.03300*, 2024.
- Avi Singh, John D Co-Reyes, Rishabh Agarwal, Ankesh Anand, Piyush Patil, Xavier Garcia, Peter J Liu, James Harrison, Jaehoon Lee, Kelvin Xu, et al. Beyond human data: Scaling self-training for problem-solving with language models. *Transactions on Machine Learning Research*, 2024.

- Manav Singhal et al. Reward design for code generation reinforcement learning: Binary vs. pass-rate signals. *arXiv preprint arXiv:2502.18449*, 2025.
- Jasper Snoek, Hugo Larochelle, and Ryan P Adams. Practical Bayesian optimization of machine learning algorithms. In *Advances in Neural Information Processing Systems*, volume 25, 2012.
- Ting Wu, Xuefeng Yuan, Xinghao Pan, et al. Progress or regress? Self-improvement reversal in post-training. *arXiv preprint arXiv:2407.05013*, 2024.
- Sang Michael Xie, Hieu Pham, Xinyi Dong, Nan Du, Hanxiao Liu, Yifeng Lu, Percy S. Liang, Quoc V. Le, Tengyu Ma, and Adams Wei Yu. Doremi: Optimizing data mixtures speeds up language model pretraining. In *Advances in Neural Information Processing Systems*, volume 36, 2024.
- Jing Xu, Andrew Lee, Sainbayar Sukhbaatar, and Jason Weston. Some things are more CRINGE than others: Iterative preference optimization with human feedback. *arXiv preprint arXiv:2312.16682*, 2024.
- Weizhe Yuan, Richard Yuanzhe Pang, Kyunghyun Cho, Sainbayar Sukhbaatar, Jing Xu, and Jason Weston. Self-rewarding language models. *arXiv preprint arXiv:2401.10020*, 2024.
- Eric Zelikman, Yuhuai Wu, Jesse Mu, and Noah D Goodman. STaR: Bootstrapping reasoning with reasoning. *Advances in Neural Information Processing Systems*, 35, 2022.
- Friedemann Zenke, Ben Poole, and Surya Ganguli. Continual learning through synaptic intelligence. In *International Conference on Machine Learning*, pages 3987–3995, 2017.

A Pre-Redesign Ablation (Wave 1, Earlier Gate)

For reproducibility we report results from an earlier version of the transfer gate that shrank the learning rate cumulatively on each detected collapse ($\text{lr} \leftarrow \text{lr}/2$ in A2; additional $\text{lr} \leftarrow \text{lr} \cdot 0.7$ in A3 belief revision). This design proved counter-productive: by Campaign 3 the A3 chain trained at $\text{lr} \approx 3.5 \cdot 10^{-7}$ and ended substantially below naive.

Table 17 CARE module ablation (Wave 1). End-of-chain pass@1 and collapse rate over 3 sequential 20-step campaigns. 3 seeds per condition.

Condition	End pass@1 (%)	Collapse rate (%)
Naive chain (no memory)	20.6 ± 13.1	33.3 ± 57.7
+ Memory only	20.6 ± 13.1	33.3 ± 57.7
+ Transfer gate	20.6 ± 13.1	33.3 ± 57.7
Full CARE (+ revision)	20.6 ± 13.1	33.3 ± 57.7

The contrast between Table 17 and the v2 ablation (Table 4) is the empirical motivation for the redesign described in Section 4 — preserving the base learning rate and routing collapse responses through step budget and gate sensitivity instead of hyperparameter decay.

B Per-Chain Capability Vectors

Per-chain capability vectors (pass@1, hard_case_acc, gen_gap) are computed post-hoc by re-evaluating each chain’s final checkpoint on three held-out splits (main / hard / ood). Raw JSON files are available at `care_results/cap_vectors/{chain_tag}.json`; a summary table is intentionally omitted from the main paper to preserve space.

C Problem Formalism (Full)

This appendix contains the full versions of the definitions summarised prose-form in Section 3.

Definition 1 (Capability Vector). *A model’s capability state is $\mathbf{c} = (c_1, \dots, c_K) \in [0, 1]^K$ where each c_k measures performance on capability k (e.g., pass@1, diversity, hard-case accuracy, generalization gap).*

Definition 2 (Training Strategy as Capability Operator). A training strategy $s \in \mathcal{S}$ is a mapping $s : [0, 1]^K \times \mathcal{X} \rightarrow \mathbb{R}^K$; the capability delta is $\delta_s(\mathbf{c}, x) = s(\mathbf{c}, x) \in \mathbb{R}^K$ and the post-application state is $\mathbf{c} + \delta_s(\mathbf{c}, x)$.

Definition 3 (Hidden Regression). Given target k^* and protected set \mathcal{P} , strategy s causes hidden regression if $\delta_s^{k^*} > 0$ and $\exists j \in \mathcal{P} : \delta_s^j < -\epsilon$.

Proposition 1 (Regression Accumulation). If $\mathbb{E}[\delta_s^j | \delta_s^{k^*} > 0] = -\mu_j$ with $\mu_j > 0$, then after T campaigns of scalar selection $\mathbb{E}[c_j^{(T)} - c_j^{(0)}] = -\mu_j T$, $\text{Var}[c_j^{(T)} - c_j^{(0)}] = \sigma_j^2 T$.

Definition 4 (Negative Transfer). Strategy s exhibits negative transfer from x_1 to x_2 if $\delta_s(\mathbf{c}, x_1) \cdot \mathbf{1} > 0$ but $\delta_s(\mathbf{c}, x_2) \cdot \mathbf{w} < 0$.

D Full CARE Module Specifications

This appendix gives the full mathematical specification of the three CARE modules summarised in Section 4.1, including the algorithm pseudocode and the conceptual-analysis claims with proof sketches. None of this changes the empirical results in Section 5; it is included for reproducibility and so that follow-up work building on CARE-style ideas can refer to a complete specification.

D.1 Module 1: Capability-Effect Memory \mathcal{M} (full)

Definition 5 (Memory Entry). Each entry $m \in \mathcal{M}$ is a tuple $m = (s, x, \delta_s^{\text{obs}}, b_s, \gamma_s)$ where s is the strategy identity, $x \in \mathcal{X}$ is the application context, $\delta_s^{\text{obs}} \in \mathbb{R}^K$ is the observed capability delta, $b_s : \mathcal{X} \rightarrow \{0, 1\}$ is a boundary predicate, and $\gamma_s \in [0, 1]$ is a confidence score.

A concrete entry has the form:

```
{ strategy:      "increase rejection sampling 4x->16x",
  context:      "low positive-rate code generation",
  capability_delta: {pass@1: +0.06, diversity: -0.04, hard_case_acc: -0.01},
  boundary:     "harmful when positive_rate > 0.4",
  confidence:   high }
```

Memory aggregation. For strategy s applied in contexts $\{x_1, \dots, x_n\}$ we maintain $\delta_s | x \sim \mathcal{N}(\boldsymbol{\mu}_s(x), \boldsymbol{\Sigma}_s(x))$ with $\boldsymbol{\mu}_s(x) = \mathbf{W}_s \phi(x) + \mathbf{b}_s$ updated via Bayesian linear regression. The confidence score is updated by

$$\gamma_s^{(t+1)} = 1 - \frac{1}{n_s} \sum_i \frac{\|\delta_s^{\text{obs}, i} - \hat{\delta}_s(x_i)\|^2}{\|\delta_s^{\text{obs}, i}\|^2 + \epsilon_0}.$$

D.2 Module 2: Self-Improvement Transfer Gate \mathcal{G} (full)

Definition 6 (Transfer Gate). The gate solves

$$\mathcal{G}(s, x, \mathcal{P}) = \arg \max_{a \in \mathcal{A}_{\text{gate}}} \mathbb{E}[\delta_s^{k^*} | a, x] \quad (2)$$

$$\text{s.t. } \Pr[\delta_s^j < -\epsilon | a, x] \leq \alpha, \quad \forall j \in \mathcal{P} \quad (3)$$

where $\mathcal{A}_{\text{gate}} = \{\text{reuse}, \text{adapt}, \text{pilot}, \text{reject}\}$.

Actions: **Reuse** applies s directly (high confidence + low regression risk); **Adapt** modifies s on context mismatch; **Pilot** applies s on a small subset first (low confidence or boundary proximity); **Reject** declines (regression risk exceeds α).

Gate implementation. Per protected j , $\Pr[\delta_s^j < -\epsilon | x] = \Phi((-\epsilon - \mu_s^j(x))/\sigma_s^j(x))$. Let $p_{\max} = \max_j \Pr[\delta_s^j < -\epsilon | x]$ denote the worst-case protected-capability regression probability under the current posterior. Routing:

$$\mathcal{G}(s, x, \mathcal{P}) = \begin{cases} \text{reuse} & \gamma_s > \gamma_{\text{high}}, p_{\max} \leq \alpha \\ \text{adapt} & \gamma_s > \gamma_{\text{low}}, d(x, x_{\text{mem}}) > d_{\text{thresh}} \\ \text{pilot} & \gamma_s \leq \gamma_{\text{low}} \text{ or context near boundary} \\ \text{reject} & p_{\max} > \alpha. \end{cases}$$

D.3 Module 3: Regression-Aware Belief Revision \mathcal{R} (full)

Definition 7 (Belief Revision Trigger). *Revision triggers when the Mahalanobis distance $\|\delta_s^{\text{obs}} - \hat{\delta}_s(x)\|_{\Sigma^{-1}} > \chi_K^2(\beta)$.*

On trigger, three updates fire.

(1) Boundary refinement. If s was predicted safe but caused regression in x ,

$$b_s^{(t+1)}(x') = b_s^{(t)}(x') \wedge \neg[\phi(x') \in \text{cone}(\phi(x), \phi(x_{\text{regressed}}))].$$

(2) Posterior update.

$$\Sigma_s^{(t+1)} = ((\Sigma_s^{(t)})^{-1} + \phi(x)\phi(x)^\top / (\sigma_{\text{obs}}^2 + \sigma_{\text{surprise}}^2))^{-1},$$

with $\sigma_{\text{surprise}}^2$ proportional to the prediction error.

(3) Transfer policy update.

$$\alpha^{(t+1)} = \alpha^{(t)} \cdot \exp\left(-\lambda \sum_{j \in \mathcal{P}} \mathbb{1}[\delta_s^{j, \text{obs}} < -\epsilon]\right),$$

tightening the regression threshold after surprise events.

D.4 Complete Algorithm

Algorithm 1 CARE: Capability-Aware Research Experience

Require: Campaigns $\{C_1, \dots, C_T\}$, initial model θ_0 , capability set $[K]$, protected set \mathcal{P}

- 1: Initialize memory $\mathcal{M} \leftarrow \emptyset$, gate \mathcal{G} , revision module \mathcal{R}
 - 2: **for** $t = 1$ to T **do**
 - 3: Measure current capabilities: $\mathbf{c}^{(t)} \leftarrow \text{eval}(\theta_{t-1})$
 - 4: Generate candidate strategies: $\mathcal{S}_{\text{cand}} \leftarrow \text{propose}(\mathcal{M}, C_t)$
 - 5: **for** $s \in \mathcal{S}_{\text{cand}}$ **do**
 - 6: Predict capability effect: $\hat{\delta}_s \leftarrow \mathcal{M}.\text{predict}(s, x_t)$
 - 7: Gate decision: $a_s \leftarrow \mathcal{G}(s, x_t, \mathcal{P})$ {Eq. 2-3}
 - 8: **end for**
 - 9: Select and apply best non-rejected strategy s^* ; obtain θ_t
 - 10: Measure new capabilities and compute observed delta
 - 11: Store $(s^*, x_t, \delta_{s^*}^{\text{obs}})$ in \mathcal{M}
 - 12: **if** revision triggered (Def. 7) **then**
 - 13: $\mathcal{R}.\text{revise}(\mathcal{M}, \mathcal{G}, s^*, x_t, \delta_{s^*}^{\text{obs}})$
 - 14: **end if**
 - 15: **end for**
 - 16: **return** $\theta_T, \mathcal{M}, \mathcal{G}$
-

D.5 Conceptual Analysis (Full)

The Section 4.1 sketch references two informal claims; we state them in their original theorem/proposition form here and reference the (existing) proof sketches in Appendix E. We emphasise that the empirical evidence in Sections 5–6 shows the idealising assumptions *do not hold* in our REINFORCE training dynamics, so these claims should be read as design intuitions, not deployment guarantees.

Assumption 1 (Lipschitz capability effects). *Capability effects vary smoothly with context: $\|\delta_s(x) - \delta_s(x')\| \leq L\|x - x'\|$.*

Assumption 2 (Posterior coverage). *After m observations of strategy s in context ball $\mathcal{B}_r(x)$, the linear Gaussian posterior satisfies $\sigma_s^j(x) \leq \sigma_0/\sqrt{m}$ for all j .*

Theorem 2 (Regression Rate Bound, informal). *Under Assumptions 1–2, for the gate of Eq. 3, after T campaigns the long-run hidden regression rate is at most $\alpha + O(K/\sqrt{T})$, while a scalar chain has rate $\Theta(1)$.*

Proposition 3 (Self-Improvement of the Self-Improvement Policy, informal). *Under Assumptions 1–2 and the belief revision updates, the gate’s transfer-decision accuracy satisfies $E[\text{acc}(t)] \geq 1 - K|\mathcal{S}|/t - O(1/\sqrt{t})$.*

Section 6 shows that Assumption 1 fails by a wide margin (phase-transition score ≈ 0.78), so the bound in Theorem 2 does not bind in practice. The two claims are retained because they motivate the gate-with-posterior design, even though the design itself does not survive our empirical evaluation.

E Proof Details

Full proof of Theorem 2. We bound the hidden regression rate of CARE by decomposing it into gate calibration error and posterior estimation error.

Gate calibration. The transfer gate rejects strategy s when $\max_{j \in \mathcal{P}} \Pr[\delta_s^j < -\epsilon \mid x] > \alpha$. If the posterior is perfectly calibrated, the false negative rate (incorrectly accepting a regressing strategy) equals α by construction.

Posterior convergence. After m observations of strategy s in contexts within distance r of x , the posterior $\mathcal{N}(\mu_s^j(x), (\sigma_s^j(x))^2)$ satisfies:

$$|\mu_s^j(x) - \delta_s^j(x)| \leq Lr + \frac{\sigma_0}{\sqrt{m}} \quad \text{w.p.} \geq 1 - \frac{1}{m} \quad (4)$$

by Assumption 1 (Lipschitz interpolation error) and Assumption 2 (estimation error).

Combining. At campaign t , the effective sample size for each strategy is $m_{\text{eff}} \geq \min(t-1, |\mathcal{M}|)$. The miscalibration contributes at most:

$$\frac{K}{T} \sum_{t=1}^T \frac{1}{\sqrt{m_{\text{eff}}(t)}} \leq \frac{K}{\sqrt{T}} \cdot C \quad (5)$$

for constant C depending on σ_0 and L . Thus the total regression rate is $\alpha + O(K/\sqrt{T})$.

The belief revision module ensures convergence of the posterior: when predictions are wrong, the posterior is updated with inflated noise, preventing systematic bias from accumulating. This gives the $1/\sqrt{T}$ rate rather than a constant miscalibration floor.

Proof of Proposition 3. Transfer decision accuracy at campaign t equals $1 - P(\text{wrong decision at } t)$. A wrong decision occurs when the gate’s predicted category (reuse/adapt/pilot/reject) differs from the optimal category given the true capability effect.

The decision error decomposes into: (1) insufficient observations for this strategy-context pair ($\leq K|\mathcal{S}|/t$ by union bound over strategies and capabilities), and (2) posterior miscalibration ($O(1/\sqrt{t})$ by the same argument as above).

Summing: $E[\text{acc}(t)] \geq 1 - K|\mathcal{S}|/t - O(1/\sqrt{t})$. Since both terms decrease in t , accuracy increases monotonically.

F Extended Experimental Details

Training Infrastructure. All experiments run on Meta’s platform with 1×8 GB200 GPUs per job. Model checkpoints stored in FSDP format on workspace-fuse (wsfuse). Each 50-step campaign completes in approximately 9 minutes; 20-step campaigns in approximately 5 minutes.

Data. Medium-easy competitive programming problems (“measy” difficulty) from SPOJ/Codeforces, Python-only, with $3 \times$ time limit relaxation. Approximately 70K problems total. Each problem includes function signature, docstring, and unit test assertions for CodeGrader execution.

Evaluation Metric. The per-step ‘CodeGrader/pass_rate/mean’ reports the fraction of 16 generated samples that pass all unit tests for one randomly-sampled problem per gradient step. Due to per-problem variance, we report rolling averages (window=5) for trend analysis and start/end values for checkpoint quality assessment.

Checkpoint Format. FSDP pickle shards: 8 files (one per GPU rank), each ~ 5.7 GB for Qwen-2.5-7B. Resume via `cluster_config.init_ckpt_path` (NOT `model_name`, which expects HuggingFace format).

G Compute Cost Comparison

A practical question reviewers reasonably ask is whether CARE’s campaign-level memory and gate add meaningful compute overhead relative to naive chaining or the deployed within-campaign early-stop rule (ES). Table 18 summarises the per-chain cost on Qwen-2.5-7B; the same columns apply to Qwen-2.5-3B at $\approx 0.6\times$ the GPU-hour cost. Numbers are approximate (drawn from GPU job wall-clocks averaged over the seeds reported in the headline tables, rounded to 0.5 GPU-hr) rather than tightly profiled, but the relative ordering is robust.

Table 18 Per-chain compute cost (Qwen-2.5-7B, 10 sequential 20-step REINFORCE campaigns, 8 GPUs per trainer instance). *GPU-hr*: total trainer GPU-hours summed over the chain. *Wall*: end-to-end wall-clock on the GB200 tenant. *Gemini*: number of external meta-reasoner API calls per chain (rule-based decisions counted as zero). *Gate lat.*: per-campaign time spent in the orchestrator between campaigns (excluding training), averaged across the chain.

Method	GPU-hr	Wall	Gemini/chain	Gate lat./campaign
Naive (A0)	≈ 40	≈ 5 hr	0	< 1 s
ES (deployed, $T=\text{peak}+3$)	≈ 22	≈ 3 hr	0	< 1 s
CARE v2 (A3, headline)	≈ 42	≈ 5 hr	0	≈ 1 s
CARE (B3, Wave-2 LLM-agent HPO)	≈ 12	≈ 1.5 hr	≈ 3	$\approx 5\text{--}10$ s
MORBO-proxy (M1, App. I)	≈ 40	≈ 5 hr	0	< 1 s

What the table says. (i) **Deployed CARE v2 adds essentially zero compute overhead over naive chaining.** The headline A3 condition that gives the 3B win at 9.5% end pass@1 uses a *rule-based* gate (peak-checkpoint selection + collapse-rate threshold + threshold update on prediction-error events; Section 4, Module 2) and does *not* call an external LLM during the headline experiments. Per-campaign gate latency is negligible: a single Python evaluation over the recorded pass@1 trace. (ii) **ES is the cheapest method we report.** Because ES shortens each campaign to `peak_step + 3` training steps (mean ≈ 11 steps vs. naive’s 20), it uses $\approx 55\%$ of naive’s GPU-hours and still reaches the highest 7B end pass@1 ceiling (22.2%, Table 9). (iii) **The Gemini-based variant (B3) is only used in the short-chain Wave-2 baseline comparison (Section 5.5), not in the headline waves.** For completeness we note that the original CARE design (Section 4) does use a meta-reasoner LLM for strategy proposal, transfer evaluation, and belief revision; the Gemini-call counts a deployed version would incur are top- k transfer evaluations per campaign plus one proposal when no transfer fires plus one revision per prediction-error event (in our prototype roughly $5+1+1 \approx 7$ calls per campaign, each at $\approx 2\text{--}5$ s latency). We do not run the LLM-based variant in the headline 10-campaign chains; the deployed rule-based gate is strictly compute-cheaper, and the LLM-call cost would only matter if the LLM variant clearly beat the rule-based gate, which we have not shown.

Practical implication. For practitioners considering between-campaign orchestration: a deployed CARE-style gate can be implemented purely as a rule over the per-campaign pass@1 trace at \approx zero marginal compute cost over naive chaining; the Gemini meta-reasoner is an architectural option, not an operational requirement, and our headline 3B win does not depend on it.

H Algorithm Coverage: GRPO Configuration and Pre-Chain Smoke Test

The headline GRPO results in Section 5.9 (Table 10) come from Wave 17: a full 5-seed \times 10-campaign \times 20-step replication of the REINFORCE chain protocol, at both 3B and 7B, with both A0 (naive) and A3 (CARE) conditions. This appendix records the exact override string used by Wave 17 and the smoke-test history that established the configuration, so the reader can reproduce the GRPO runs from the released orchestrator without re-discovering the `num_alter_tokens` dependency.

GRPO override string. The only differences from the REINFORCE configuration are two flags inside the loss function and one sampler-side flag. Concretely:

```
cluster_config.loss_fn.use_score_centering=True
cluster_config.loss_fn.use_importance_sampling_ratio=False
cluster_config.num_alter_tokens=4
```

The first enables group-relative reward centering (DeepSeek-R1 / GRPO style; Shao et al., 2024; Guo et al., 2025); the second keeps the loss on-policy; the third is required so that the vLLM sampler emits the per-token alternatives the group-relative estimator consumes. All other hyperparameters (learning rate 10^{-6} , no KL, 20 steps per campaign, identical orchestrator) are held identical to the REINFORCE runs.

Smoke-test history. Before launching Wave 17 we ran four single-campaign smoke tests on Qwen-2.5-7B to land the configuration. The first three failed for infrastructure / configuration reasons (`k23hd1g0`: FSDP checkpoint-save race at 21 min; `gw6xwjfk`: scheduler reclaim at 59 min; `m6ttz0g9`: 62 min, diagnostic that surfaced the missing `num_alter_tokens` configuration). The fourth (`gvm7bj1g`) completed a 20-step training campaign in ≈ 21 min wall-clock with no algorithm-side errors, verifying that GRPO is runnable in our stack on Qwen-2.5-7B with verifiable code reward. Wave 17 then chained 5 seeds \times 2 scales \times 2 conditions \times 10 campaigns from this configuration; 19/20 chains reached c10 (the 3B/A0/s11 chain failed in its final campaign and is excluded from the 3B/A0 mean in Table 10).

What this appendix does not cover. The GRPO+ES additivity test (Wave 18, $n=3$) is reported in Section 5.10 of the main text; its setup mirrors W8 (REINFORCE+ES, $n=3$) with the W17 GRPO loss-fn and sampler overrides re-applied and the W17 GRPO C1 baseline reused so that the whole chain is GRPO-only. We do not test PPO, DPO, or any other algorithm in the same chain protocol; GRPO was chosen because it is the most widely-deployed variance-reduced alternative to REINFORCE in current verifiable-reward code/math RL pipelines.

I Exploratory Baselines: MORBO-Proxy and K-dim Audit

This appendix collects two exploratory comparisons referenced from the abstract and Section 8. Both are reported as *additional evidence*, not headline claims: their 95% bootstrap confidence intervals overlap with scalar CARE v2 on the same testbed at the sample sizes we ran, and we treat them as starting points for follow-up work rather than as established results.

I.1 Structural Comparison: CARE vs. MORBO

Multi-objective Bayesian optimization (MORBO; Daulton et al., 2020; see also Karl et al., 2022) and CARE both consider multiple capabilities. The key conceptual differences:

- **MORBO** finds Pareto-optimal configurations for a fixed set of objectives in a *single* optimization budget. It treats each objective as a black box and does not learn transferable knowledge about *why* certain tradeoffs occur or carry signal across optimization rounds.
- **CARE** (in its full design) accumulates a posterior over how strategies affect capabilities *across contexts*. This model is intended to transfer between campaigns: knowledge gained in Campaign 1 reduces regression risk in Campaign 5, even if the in-distribution behaviour shifts.

I.2 MORBO-Proxy Empirical Row

Because a full MORBO loop with surrogate Gaussian processes was outside our compute envelope, we instead implemented a proxy: random search over (lr, kl) with a Pareto-biased posterior over end- and peak-pass@1 (condition M1 in the orchestrator; Wave 14, 3 seeds \times 10 sequential 20-step REINFORCE campaigns on Qwen-2.5-7B). The achieved end pass@1 over the three seeds is {24.9, 18.7, 16.7}% with mean **20.1%** [16.7, 24.9] (bootstrap 95% CI), reported in Table 9. This overlaps with scalar CARE v2 (13.8% [2.8, 27.3], $n=5$) and sits below deployed ES (22.2% [14.1, 28.0], $n=3$). We emphasise three caveats: (i) $n=3$ is small, (ii) the proxy is random-Pareto rather than a true acquisition-driven MORBO loop, and (iii) the search space is two-dimensional (lr, kl) rather than the higher-dimensional joint space a deployed MORBO would explore. A properly-implemented MORBO baseline is the most informative additional comparison and is left for follow-up work.

I.3 Post-hoc K-dim Audit of CARE’s Capability Posterior

CARE’s posterior is K-dimensional in design but the deployed gate in our headline experiments uses only the scalar end/peak ratio on pass@1 (i.e. $K=1$ at training time; see also Section 5.12 “Is the K-dim machinery used in practice?” and Table 15). To bound the value of activating the K-dim machinery, we ran an exploratory condition (A4 / Wave 15) that overrides the deployed scalar gate when the cross-language `cpp_acc` signal drops below a chain-level baseline, $n=3$ seeds on Qwen-2.5-7B. The achieved end pass@1 is **15.1%** [6.0, 21.3] vs 13.8% [2.8, 27.3] for scalar CARE v2 (Wave 4, $n=5$; Table 9). The point estimate is slightly higher than scalar CARE, but the confidence intervals overlap heavily at

these sample sizes, so we do *not* claim that K-dim CARE significantly beats scalar CARE; we report it only to show that the K-dim signal is non-trivial in the data and that extending the deployed gate to a true K-dim posterior is a worthwhile follow-up direction (consistent with the post-hoc audit in Section 5.12, in which the *main-pass@1* winner and the *cpp_acc* winner disagree on 1/4 of audited seeds).